Energy Harvesting: introduction

NiPS Summer School

July 7-12th, 2015

Fiuggi, Italy

Francesco Cottone

NiPS lab, Physics Dep., Università di Perugia, Italy

francesco.cottone at unipg.it

Summary

- Energy harvesting applications and principles
- Fundamentals of vibration energy harvesters
- Beyond linear systems: linear and nonlinear approaches
- Conclusions

Energy harvesting applications

Wireless Sensor Networks

Structural Monitoring

02/07/2014 - Belo Horizonte (Brazil)
(birdge collapse at FIAT factory)

Environmental Monitoring

Transportation

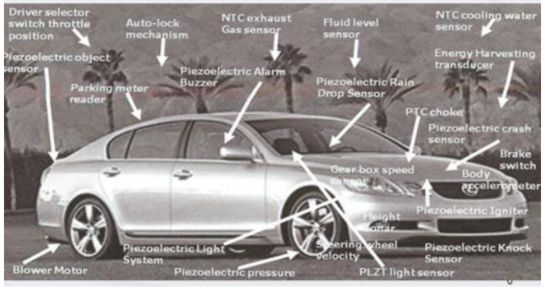

Wearable sensing for health applications

Emergency medical response
Monitoring, pacemaker, defibrillators

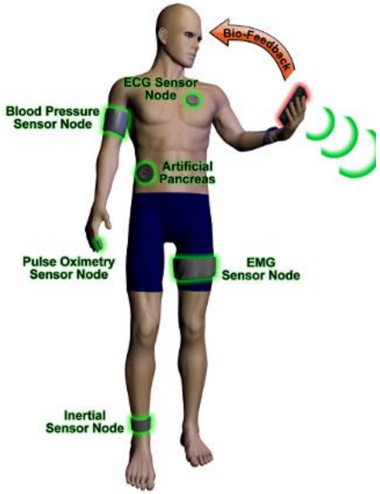

Military applications

Energy Harvesting could enable 90% of WSNs applications (IdTechex)

Power sources available from the ambient

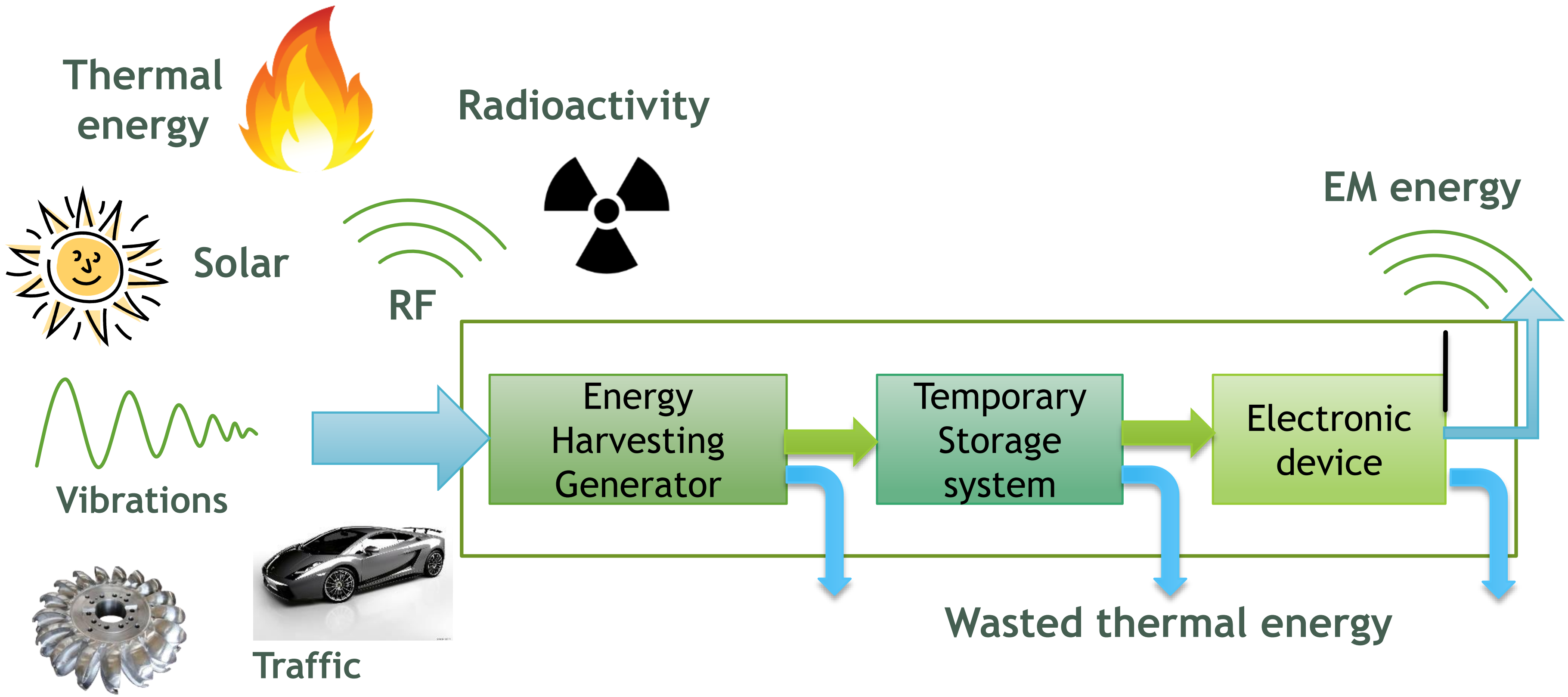

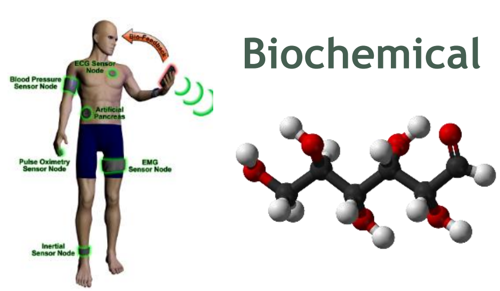

- Piezoelectric
- Electrodynamics
- Photovoltaic
- Hydro Turbine

- Ultra capacitors
- Rechargeable Batteries

- Wireless Sensor Node

Examples of energy harvesting systems

Tree - vegetation

Sailing ship (XVI-XVII century)

Crystal radio - 1906

First automatic wristwatch, Harwood, c. 1929 (Deutsches Uhrenmuseum, Inv. 47-3543)

First automatic watch.
Abraham-Louis Perrelet,
Le Locle. 1776

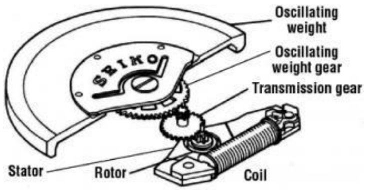

Self-charging Seiko wristwatch

Vibration energy harvesting versus power requirements

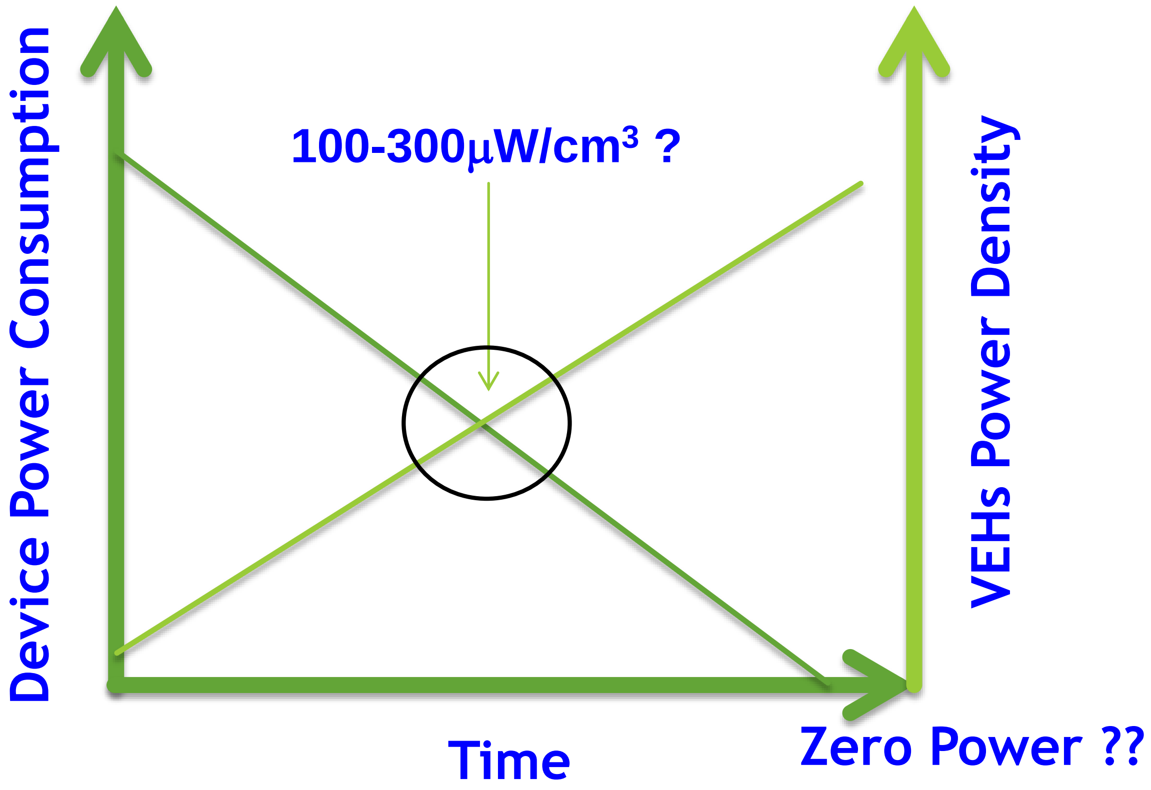

Vibration Energy Harvesters (VEHs): basics

zinc oxide (ZnO) nanowires
Wang et al. 2008

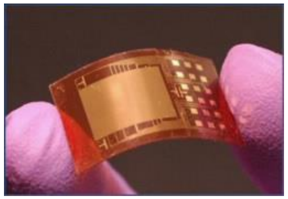

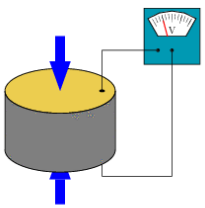

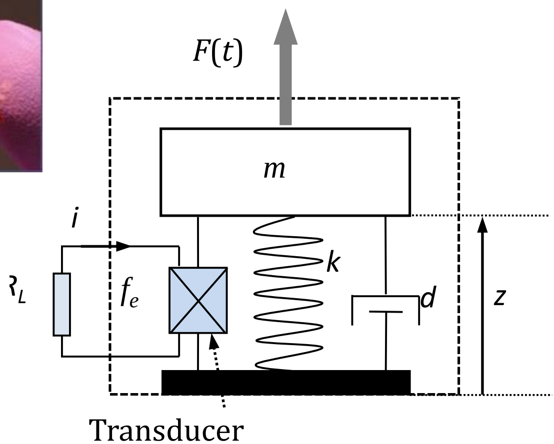

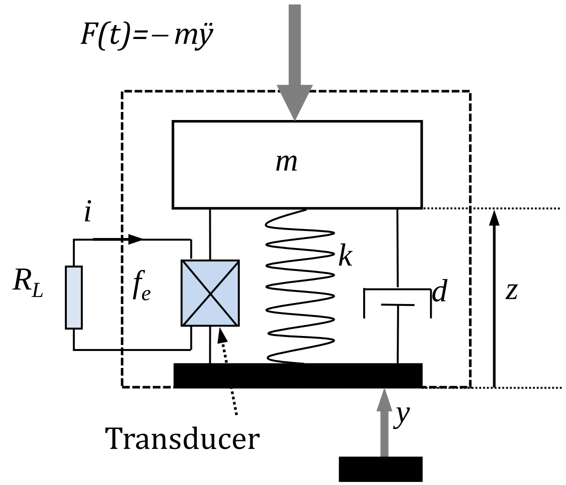

Energy harvesting from
moth vibrations
Chang. MIT 2013

Energy Harvesting from dancing

Inertial generators are more flexible than direct-force devices because they require only one point of attachment to a moving structure, allowing a greater degree of miniaturization.

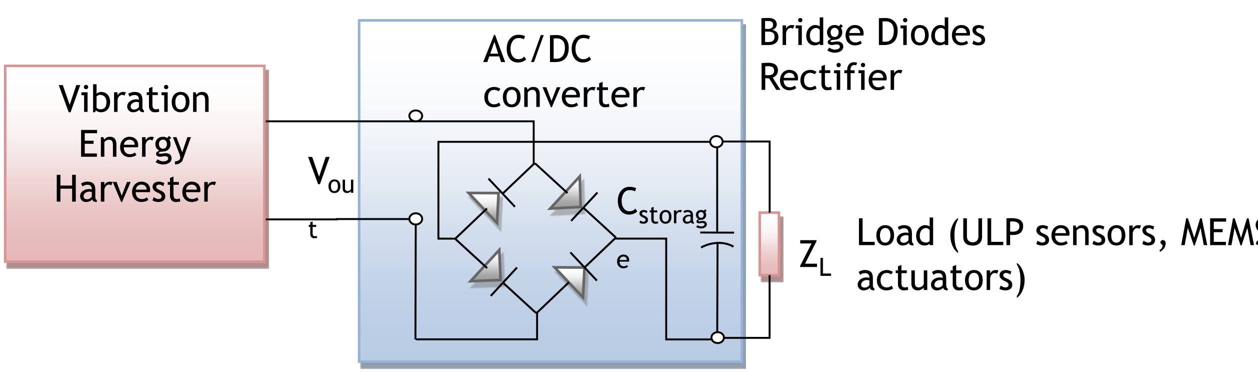

Vibration Energy Harvesters (VEHs): basics

Electromagnetic

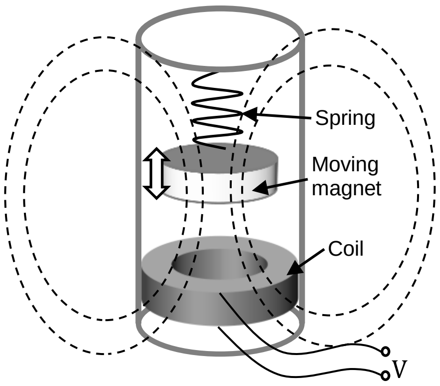

Electrostatic/Capacitive

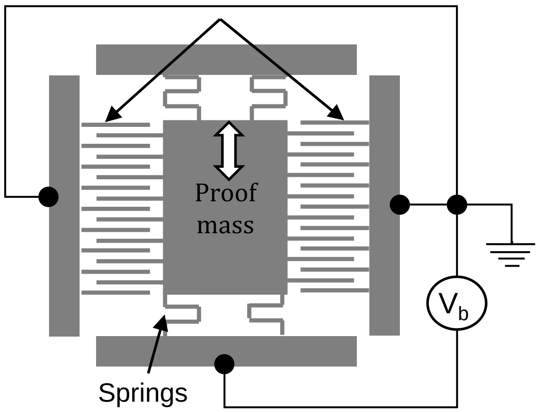

Vibration Harvesting Generator

Magnetostrictive

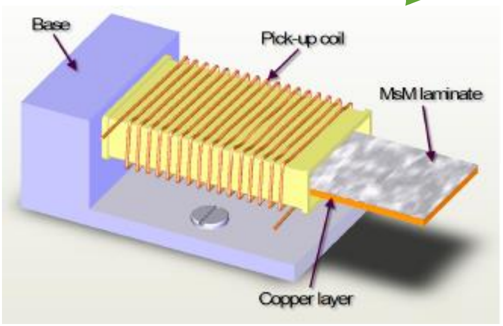

Piezoelectric

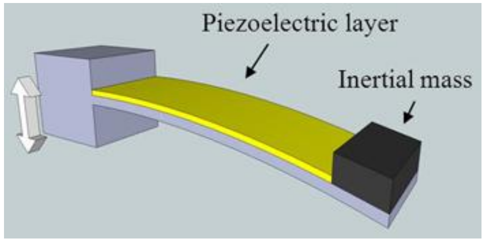

Piezoelectric conversion

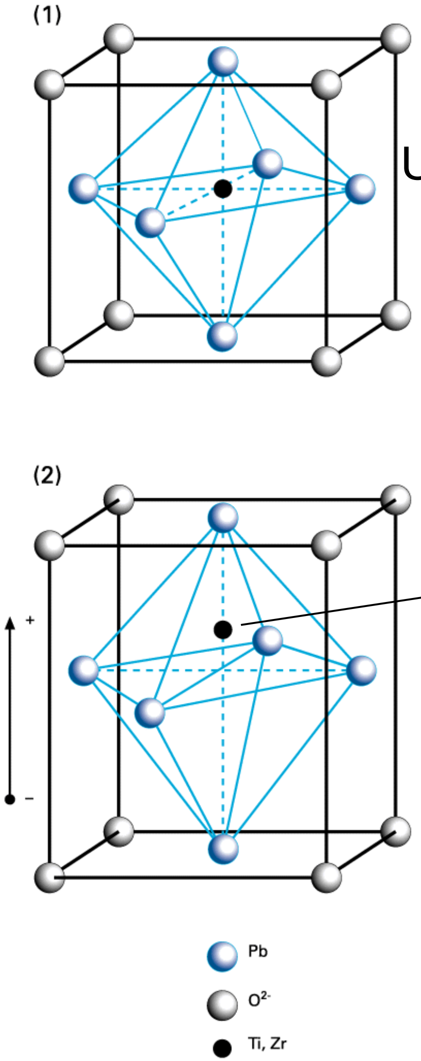

Unpolarized Crystal

Polarized Crystal

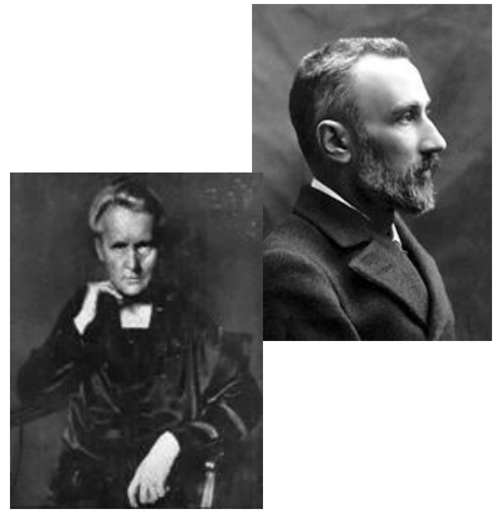

Pioneering work on the direct piezoelectric effect (stress-charge) in this material was presented by Jacques and Pierre Curie in 1880

In 1903 Pierre received the Nobel Prize in Physics with his wife, Marie Skłodowska-Curieand and Henri Becquerel, for the research on the radiation phenomena discovered by Professor Henri Becquerel.

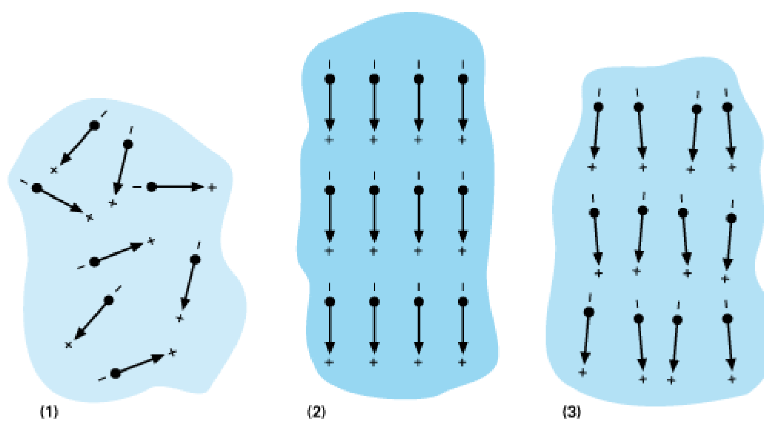

After poling the zirconate-titanate atoms are off center.
The molecule becomes elongated and polarized

Piezoelectric conversion

Stress-to-charge conversion

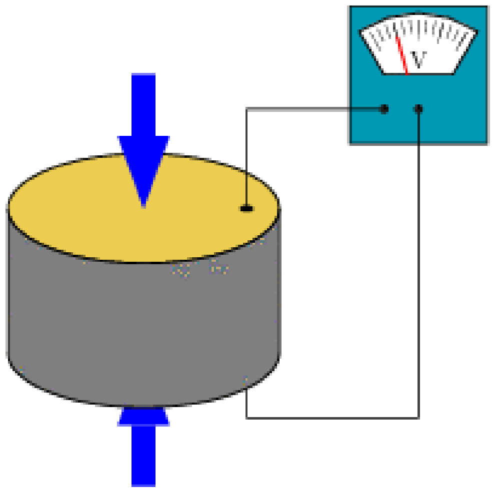

direct piezoelectric effect

Biological

- Bones
- DNA !!!

Naturally-occurring crystals

- Berlinite ($AlPO_4$), a rare phosphate mineral that is structurally identical to quartz
- Cane sugar
- Quartz (SiO_2)
- Rochelle salt

Man-made ceramics

- Barium titanate ($BaTiO_3$)—Barium titanate was the first piezoelectric ceramic discovered.
- Lead titanate ($PbTiO_3$)
- Lead zirconate titanate ($Pb[Zr_xTi_{1-x}]O_3$ $0 \le x \le 1$)—more commonly known as ***PZT***, lead zirconate titanate is the most common piezoelectric ceramic in use today.
- Lithium niobate ($LiNbO_3$)

Polymers

- Polyvinylidene fluoride (PVDF): exhibits piezoelectricity several times greater than quartz. Unlike ceramics, long-chain molecules attract and repel each other when an electric field is applied.

Piezoelectric conversion

33 Mode

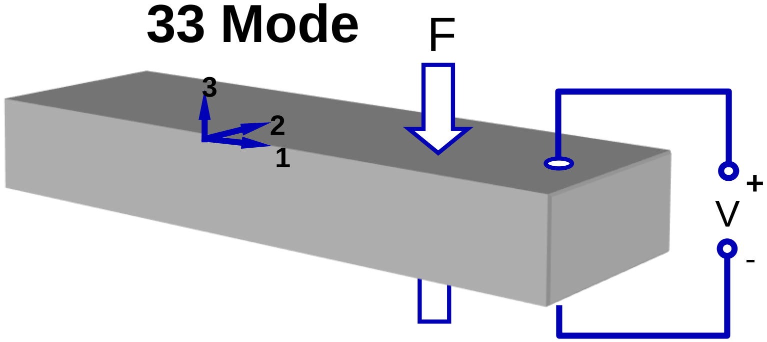

31 Mode

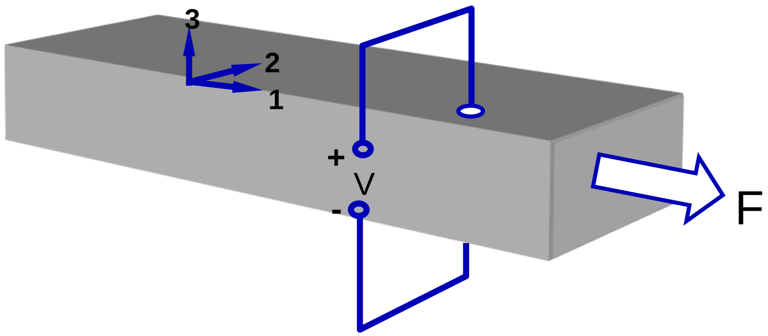

$$S = [s_E]T + [d^t]E$$
$$D = [d]T + [\varepsilon_T]E$$

Strain-charge

$$T = [c^E]S - [e^t]E$$
$$D = [e]S + [\varepsilon^S]E$$

Stress-charge

- S = strain vector (6x1) in Voigt notation
- T = stress vector (6x1) [N/m^2]
- s_E = compliance matrix (6x6) [m^2/N]
- c^E = stifness matrix (6x6) [N/m^2]
- d = piezoelectric coupling matrix (3x6) in Strain-Charge [C/N]
- D = electrical displacement (3x1) [C/m^2]
- e = piezoelectric coupling matrix (3x6) in Stress-Charge [C/m^2]
- ε = electric permittivity (3x3) [F/m]
- E = electric field vector (3x1) [N/C] or [V/m]

Conversion techniques comparison

Technique	Advantages	Drawbacks
Piezoelectric	• high output voltages • well adapted for miniaturization • high coupling in single crystal • no external voltage source needed	• expensive • small coupling for piezoelectric thin films • large load optimal impedance required (MΩ) • Fatigue effect
Electrostatic	• suited for MEMS integration • good output voltage (2-10V) • possiblity of tuning electromechanical coupling • Long-lasting	• need of external bias voltage • relatively low power density at small scale
Electromagnetic	• good for low frequencies (5-100Hz) • no external voltage source needed • suitable to drive low impedances	• inefficient at MEMS scales: low magnetic field, micro-magnets manufacturing issues • large mass displacement required.

Example of vibration sources

Human activity

Scenario	$\overline{P}$
Taking a book off a shelf	<10 μW
Putting on reading glasses	<10 μW
Reading a book	<10 μW
Writing with a pencil	10–15 μW
Opening a drawer	10–30 μW
Spinning in a swivel chair	<10 μW
Opening a building door	<1 μW
Shaking an object	>3,000 μW

Activity	Sensing unit placement	# subjects	Median f_m (Hz)	$\overline{P}$ (μW) [illegible]ercentile	Median	75th percentile	Median r (Kb/s)
Relaxing	Trouser pocket	42	N/A	[illegible]	3.1	4.8	0.6
	Waist belt	42	N/A	[illegible]	2.4	4.8	0.5
	Trouser pocket	42	N/A	[illegible]	1.4	5.9	0.3
Walking	Shirt pocket	42	1.9	[illegible]	155.2	186.0	31.0
	Waist belt	42	2.0	[illegible]	180.3	[illegible]	36.0
	Trouser pocket	42	2.0	[illegible]	202.4	[illegible]	40.4
Running	Shirt pocket	42	2.8	[illegible]	813.3	910.0	162.6
	Waist belt	41	2.8	[illegible]	678.3	752.8	135.6
	Trouser pocket	42	2.8	[illegible]	612.7	[illegible]	122.5
Cycling	Shirt pocket	30	3.5	[illegible]	52.0	[illegible]	10.4
	Waist belt	29	3.8	[illegible]	45.4	[illegible]	9.1
	Trouser pocket	30	1.1	[illegible]	41.3	59.5	8.3

1.9
2.0
2.0
2.8
2.8
2.8
3.5
3.8
1.1

813.3

678.3

Gorlatova, M et al (2013). Movers and shakers: Kinetic energy harv[illegible]nternet of things.

Example of vibration sources

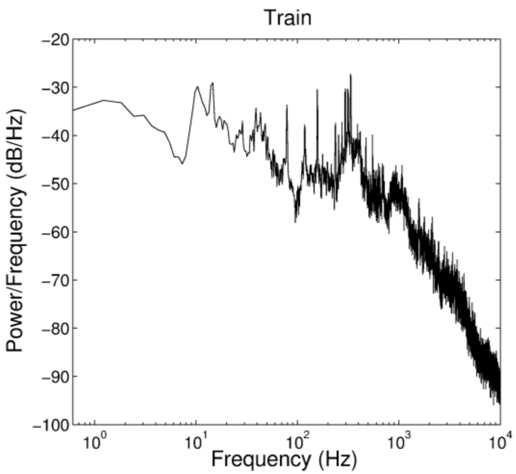

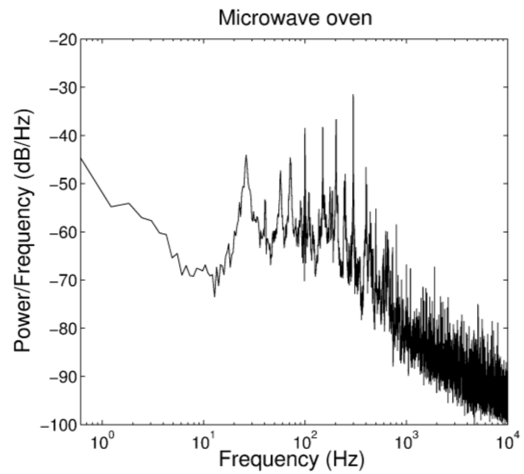

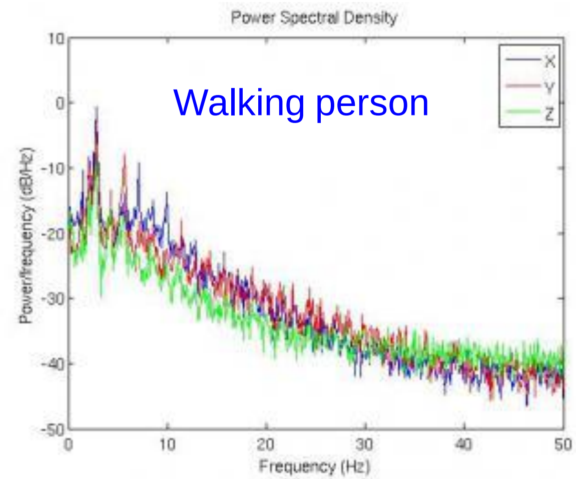

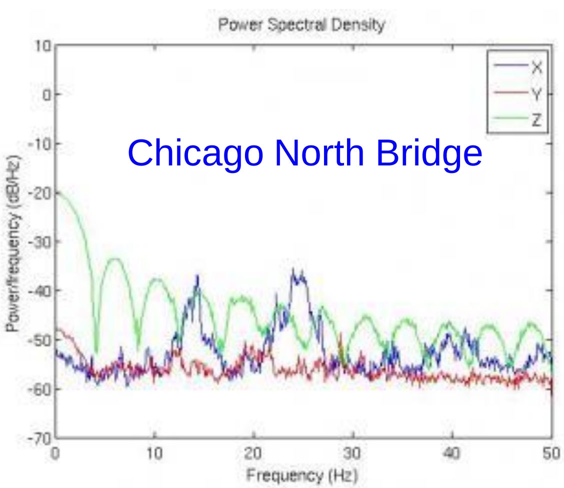

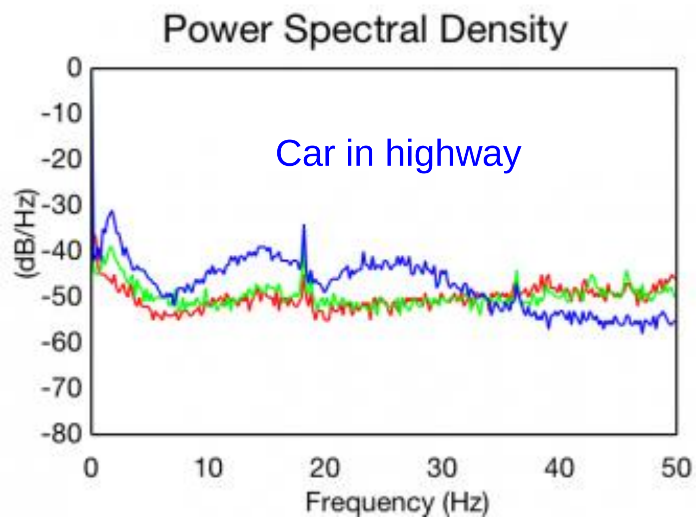

http://realvibration.nipslab.org

A general model for VEHs

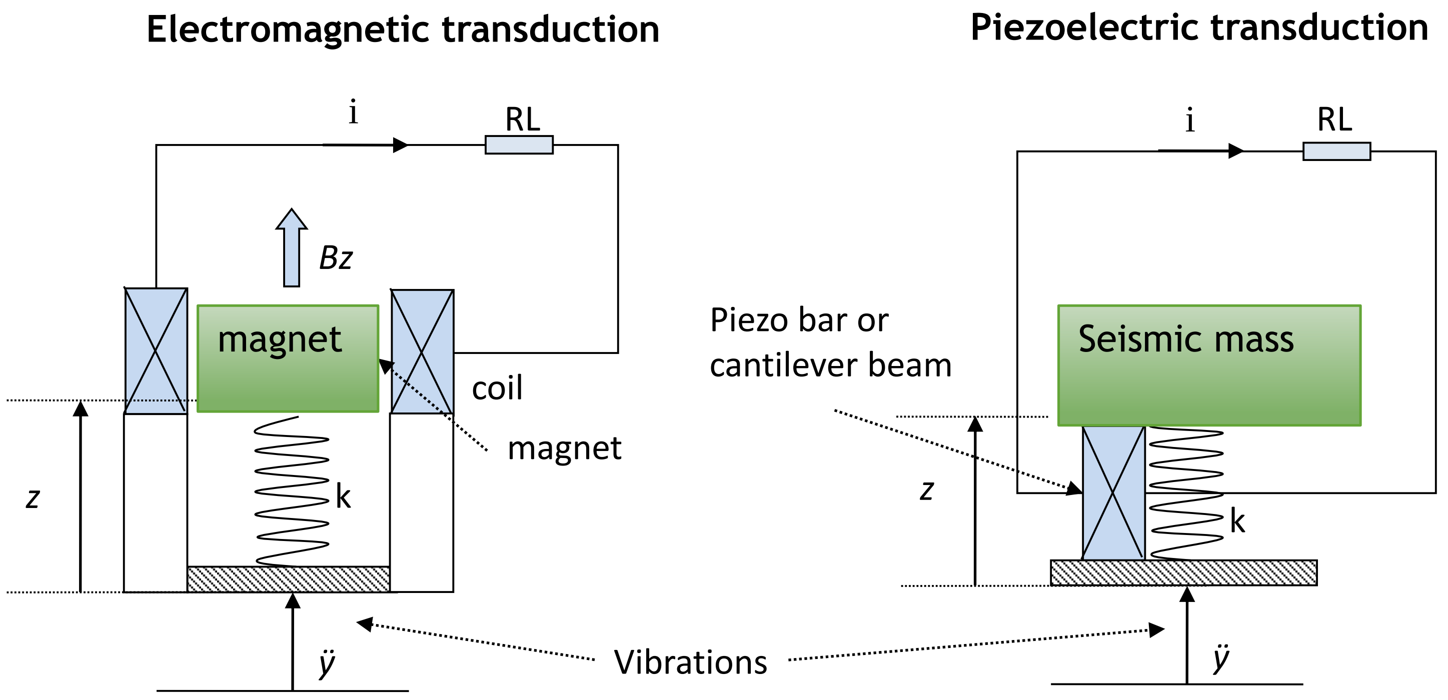

$$\begin{cases} m\ddot{z} + d\dot{z} + \dfrac{dU(z)}{dz} + \alpha V_L = -m\ddot{y} \\ \dot{V}_L + (\omega_c + \omega_i)V_L = \lambda \omega_c \dot{z} \end{cases}$$

A general model for VEHs

LINEAR mechanical oscillator $U(z) = \frac{1}{2}kz^2$ $\Rightarrow$

$$\boxed{\begin{cases} m\ddot{z} + d\dot{z} + kz + \alpha V_L = -m\ddot{y} \\ \dot{V}_L + (\omega_c + \omega_i)V_L = \lambda\omega_c\dot{z} \end{cases}}$$

Laplace transform

$$\ddot{y} = Y_0 e^{j\omega t} \Rightarrow \begin{pmatrix} ms^2 + ds + k & \alpha \\ -\lambda\omega_c s & s + \omega_c \end{pmatrix}\begin{pmatrix} Z \\ V \end{pmatrix} = \begin{pmatrix} -mY \\ 0 \end{pmatrix}$$

$$\Rightarrow \quad Z = \frac{-mY}{\det A}(s+\omega_c) = \frac{-mY\cdot(s+\omega_c)}{ms^3 + (m\omega_c + d)s^2 + (k + \alpha\lambda\omega_c + d\omega_c)s + k\omega_c},$$

$$V = \frac{-mY}{\det A}\lambda\omega_c s = \frac{-mY\cdot\lambda\omega_c s}{ms^3 + (m\omega_c + d)s^2 + (k + \alpha\lambda\omega_c + d\omega_c)s + k\omega_c}.$$

Hence, the transfer functions between displacement and voltage over input acceleration are given by

$$H_{ZY}(s) = \frac{Z}{Y}, \quad \text{(a)} \qquad H_{VY}(s) = \frac{V}{Y}. \quad \text{(b)}$$

By substituting s=jω in , we can calculate the electrical power dissipated across the resistive load

$$\Rightarrow \quad \boxed{P_e(\omega) = \frac{Y_0^2}{2R_L}\left|\frac{m_2\lambda\omega_c j\omega}{(\omega_c + j\omega)(-m_2\omega^2 + d_2 j\omega + k_2) + \alpha\lambda\omega_c j\omega}\right|^2}$$

Piezoelectric conversion

Strain-charge

$$\mathbf{S} = \mathbf{s_E} \cdot \mathbf{T} + \mathbf{d}^t \cdot \mathbf{E}$$

$$\mathbf{D} = \mathbf{d} \cdot \mathbf{T} + \boldsymbol{\varepsilon}_\mathbf{T} \cdot \mathbf{E}$$

Stress-charge

$$\mathbf{T} = \mathbf{c_E} \cdot \mathbf{S} - \mathbf{e}^t \cdot \mathbf{E}$$

$$\mathbf{D} = \mathbf{e} \cdot \mathbf{S} + \boldsymbol{\varepsilon}_\mathbf{S} \cdot \mathbf{E}$$

Characteristic	PZT-5H	BaTiO3	PVDF	AlN (thin film)
d_{33} (10^{-10} C/N)	593	149	-33	5,1
d_{31} (10^{-10} C/N)	-274	78	23	-3,41
k_{33}	0,75	0,48	0,15	0,3
k_{31}	0,39	0,21	0,12	0,23
ε_r	3400	1700	12	10,5

$$k_{31}^2 = \frac{El.energy}{Mech.energy} = \frac{d_{31}^2}{s_{11}^E \varepsilon_{33}^T}$$

Electromechanical Coupling is an adimensional factor that provides the effectiveness of a piezoelectric material. IT's defined as the ratio between the mechanical energy converted and the electric energy input or the electric energy converted per mechanical energy input

Piezoelectric conversion

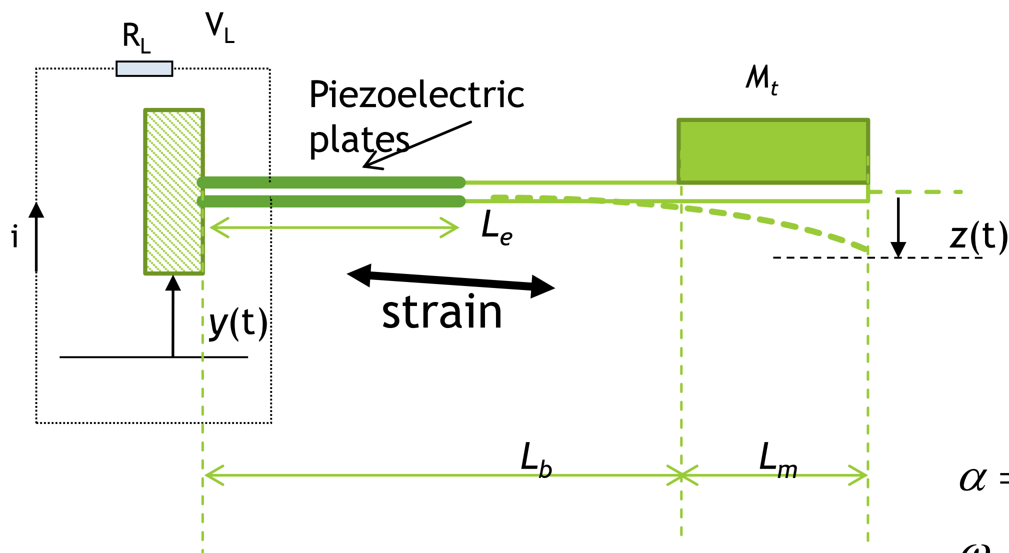

$$\begin{cases} m\ddot{z} + d\dot{z} + kz + \alpha V_L = -m\ddot{y} \\ \dot{V}_L + (\omega_c + \omega_i)V_L = \lambda \omega_c \dot{z} \end{cases}$$

$$\alpha = kd_{31} / h_p k_2, \qquad \lambda = \alpha R_L,$$

$$\omega_c = 1 / R_L C_p, \qquad \omega_i = 1 / R_i C_p,$$

Ep and *Es* are the Young's modulus of piezo layer and steel substrate respectively

$$k = k_1 k_2 E_p,$$

$$k_1 = \frac{2I}{b(2l_b + l_m - l_e)}, \qquad k_2 = \frac{3b(2l_b + l_m - l_e)}{l_b^{\,2}\left(2l_b + \frac{3}{2}l_m\right)},$$

$$b = \frac{h_s + h_p}{2}, \qquad I = 2\left[\frac{w_b h_p^3}{12} + w_b h_p b^2\right] + \frac{E_s / E_p w_b h_s^3}{12},$$

Electromagnetic conversion

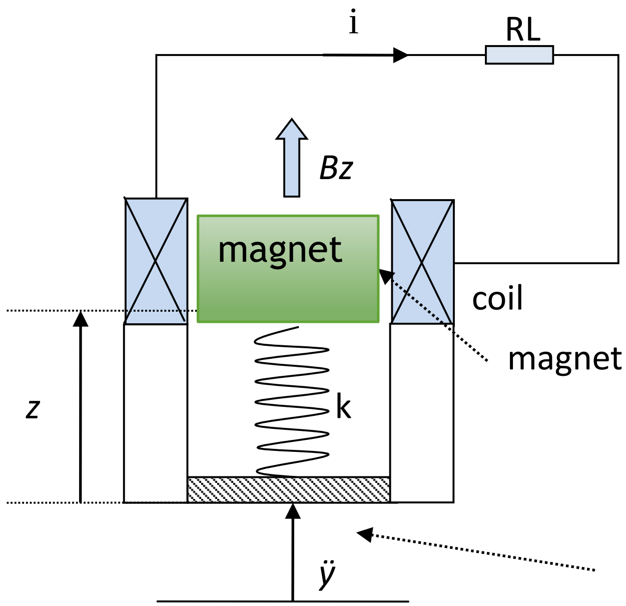

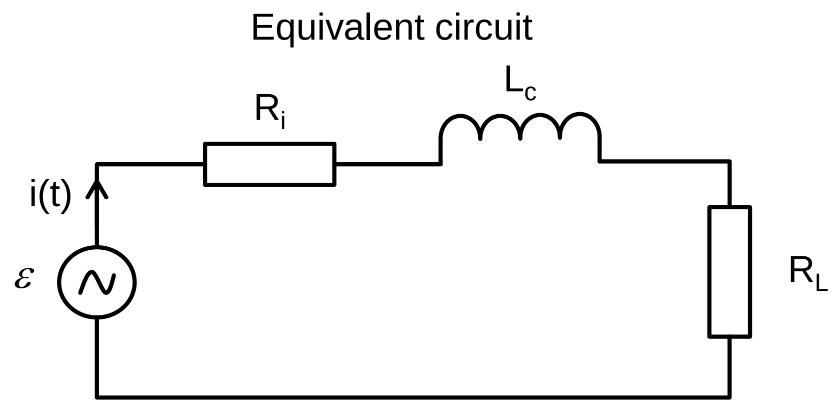

$$
\begin{cases}
m\ddot{z} + d\dot{z} + kz + \alpha V_L = -m\ddot{y} \\
\dot{V}_L + (\omega_c + \omega_i)V_L = \lambda\omega_c\dot{z}
\end{cases}
$$

$$\alpha = Bl / R_L, \qquad \lambda = Bl = \alpha R_L,$$

$$\omega_c = R_L / L_c, \qquad \omega_i = R_i / L_c,$$

MEMS electrostatic kinetic energy harvester

Mathematical modeling

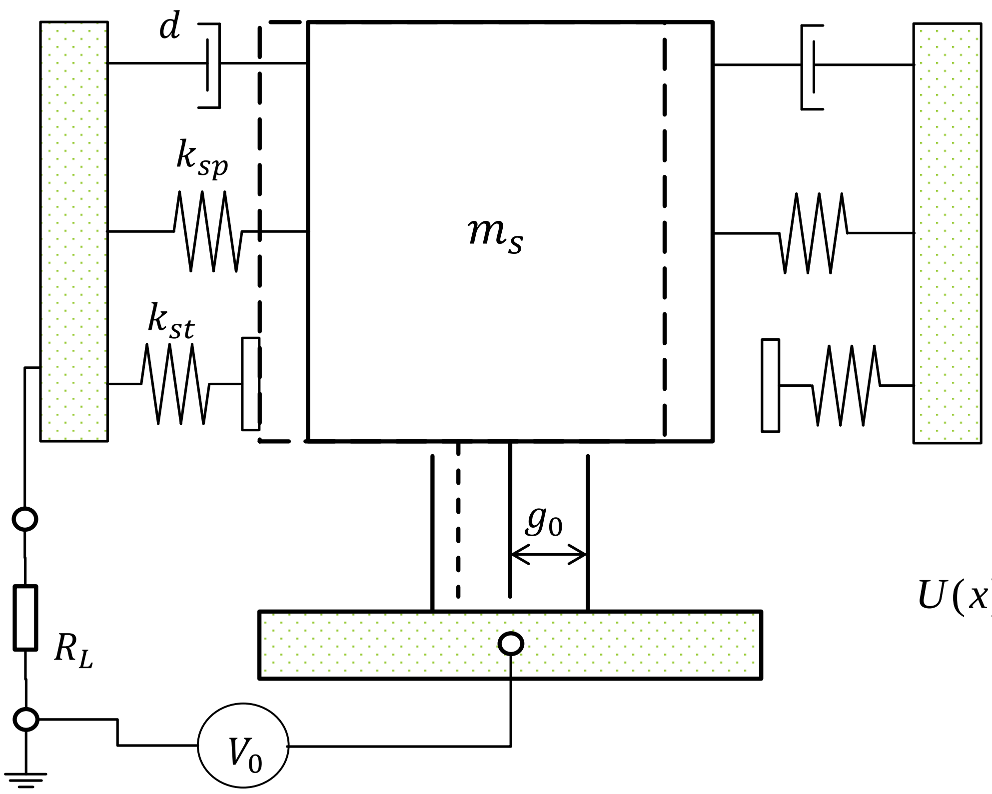

Governing equations

$$m\frac{d^2x}{dt^2}+\left(c_a+c_i\right)\frac{dx}{dt}+\frac{dU(x)}{dx}=-m\frac{d^2y}{dt^2},$$

$$R_L\frac{d}{dt}(C\cdot V)+V=U_0,$$

$$U(x)=\begin{cases}\frac{1}{2}k_{sp}x^2-\frac{1}{2}C(x)U_0^2, & \text{for } |x|<x_{\lim}\\ \frac{1}{2}(k_{sp}+k_{st})x^2-\frac{1}{2}C(x)U_0^2, & \text{for } |x|\geq x_{\lim}\end{cases}$$

Main limits of resonant VEHs

- narrow bandwidth that implies constrained resonant frequency-tuned applications
- Non-adaptation to variable vibration sources
- small inertial mass and high resonant frequency at micro/nano-scale -> most of vibration sources are below 100 Hz

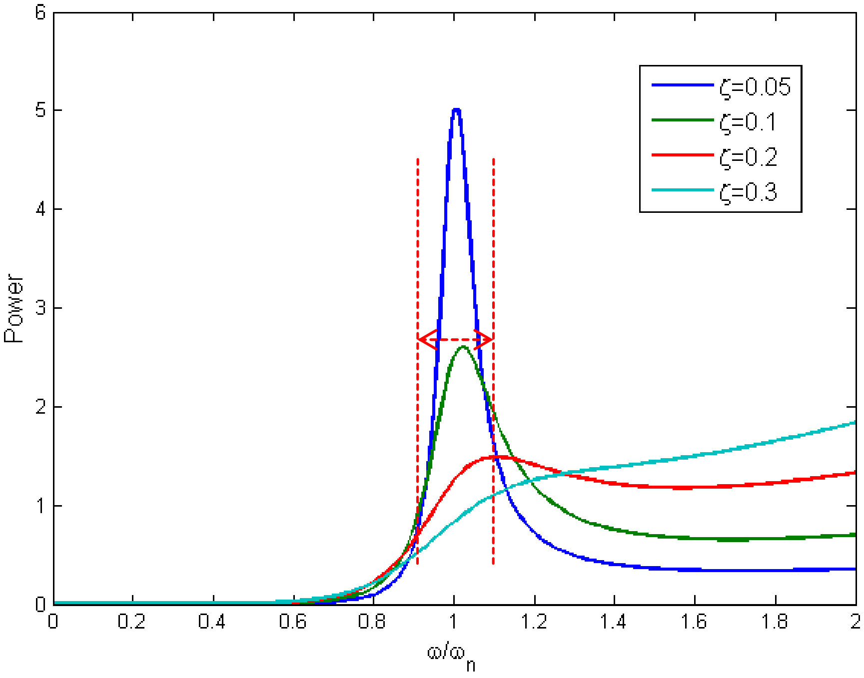

At 20% off the resonance the power falls by 80-90%

Beyond linear harvesting systems

Frequency tuning

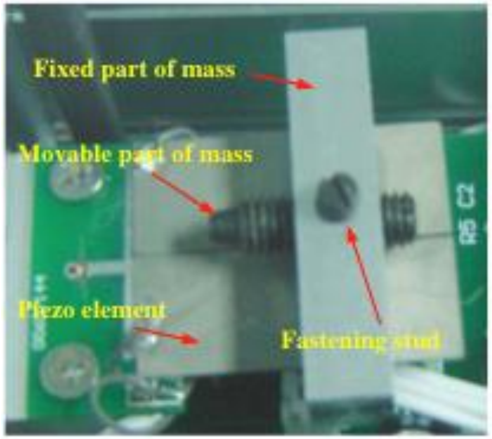

Piezoelectric cantilever with a movable mass

Wu et al. 2008

Piezoelectric cantilever with magnetic tuning

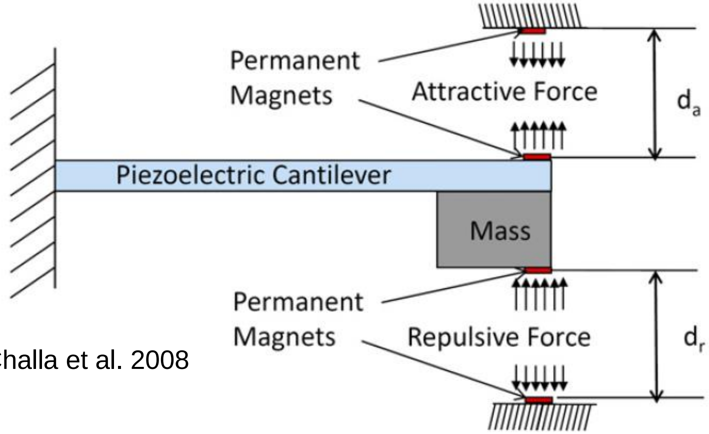

Challa et al. 2008

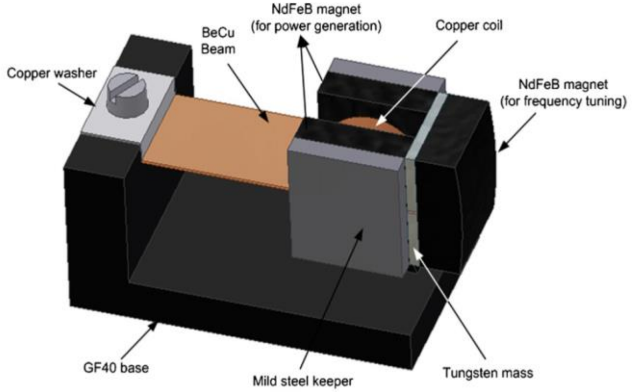

Zhu, et al. (2010). *Sensors and Actuators A: Physical*

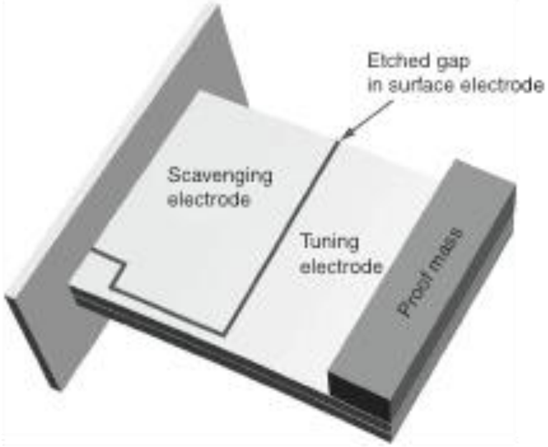

Piezoelectric beam with a scavenging and a tuning part

Roundy and Zhang 2004

Beyond linear harvesting systems

Frequency tuning

Table 2. Summary of the reported resonance tuning methods.

Author	Methods	Tuning range (Hz)	Tunability, $\left(\frac{\text{frequency change}}{\text{average frequency}}\right)$ (%)	Tuning load (force, distance, and voltage)	Energy or power for tuning	Automatic controller
Leland and Wright (2006)	Mechanical (passive)	200–250 (7.1 g tip mass)	22.22	Up to 65 N	–	×
Eichhorn et al. (2008)	Mechanical (passive)	292–380	26.19	Up to 22.75 N	–	×
Hu et al. (2007)	Mechanical (passive)	58.1–169.4	97.85	−50–50 N	–	×
Morris et al. (2008)	Mechanical (passive)	80–235 (can be wider)	≥98.41	≈1.25 mm	–	×
Loverich et al. (2008)	Mechanical (passive)	56–62	10.17	0.5 mm	–	×
Wu et al. (2008)	Mechanical (passive)	130–180	32.26	21 mm	–	×
Challa et al. (2008)	Magnetic (passive)	22–32	37.04	3 cm	85 mJ	×
Reissman et al. (2009)	Magnetic (passive)	88–99.38	12.15	1.5 cm	–	×
Zhu et al. (2008)	Magnetic (passive)	67.6–98	36.71	3.8 mm	2.04 mJ/mm	√
Wu et al. (2006)	Piezoelectric (active)	91.5–94.5	3.23	–	µW level (for controller)	√
Peters et al. (2009)	Piezoelectric (active)	66–89 (actuator PL140)	29.68	±5 V	150 mW (discrete control circuit)	√
Roundy and Zhang (2005)	Piezoelectric (active)	64.5–67	3.80	5 V	440 µW	×
Wischke et al. (2010)	Piezoelectric (semi-passive)	20 (10 mm long electrode)	≈6.7	−65 to +130 V	200 µJ	×

Tang et al. 2010

Beyond linear harvesting systems

Multimodal Energy Harvesting

Tadesse et al. 2009

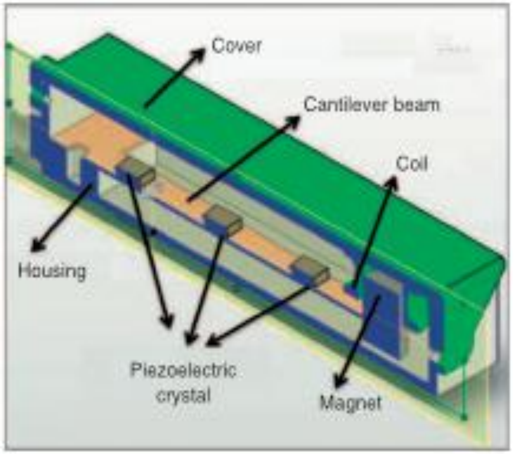

Hybrid harvester with piezoelectric and electromagnetic transduction mechanisms

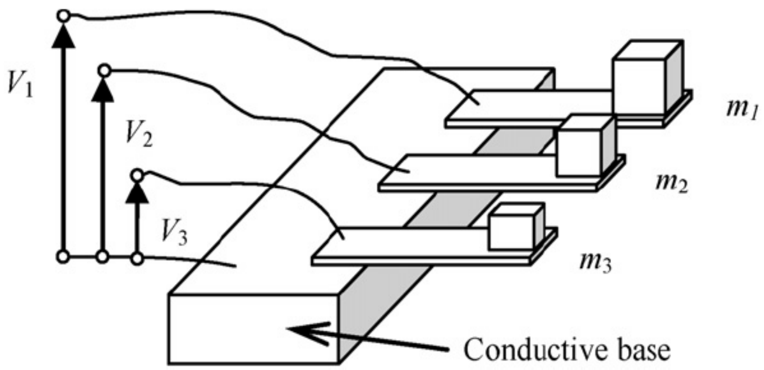

Ferrari, M., et al. (2008). *Sensors and Actuators A: Physical*

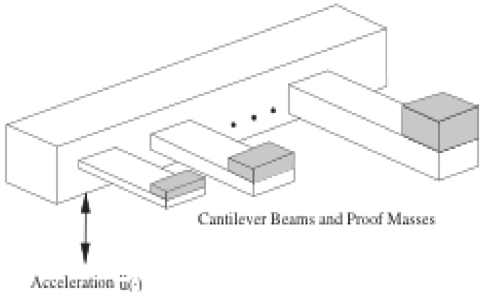

Shahruz 2006

Piezoelectric cantilever arrays
with various lengths and tip masses

Beyond linear harvesting systems

Frequency-up conversion

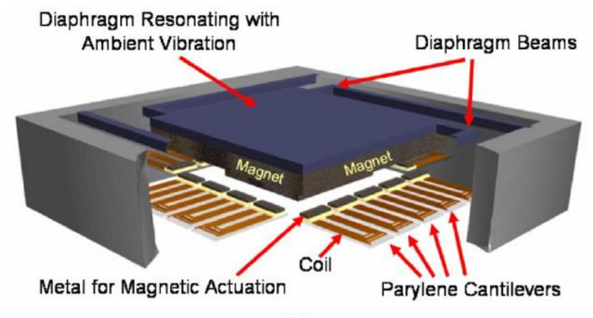

H. Kulah and K. Najafi, IEEE Sensors Journal **8** (3), 261 (2008).

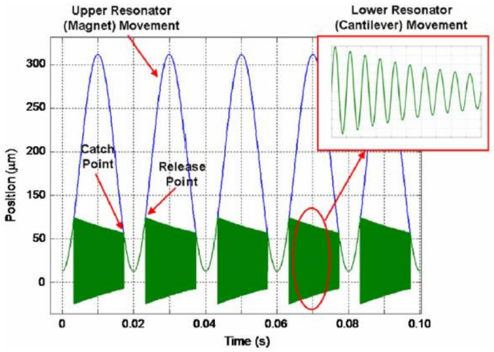

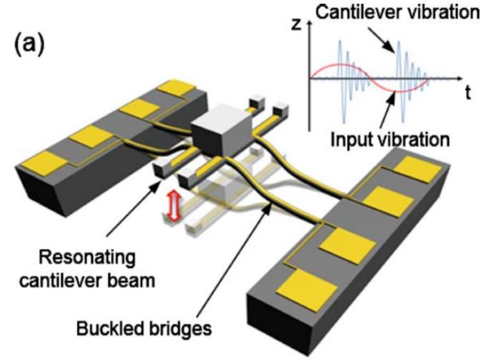

Jung, S.-M. et al. (2010). *Applied Physics Letters*

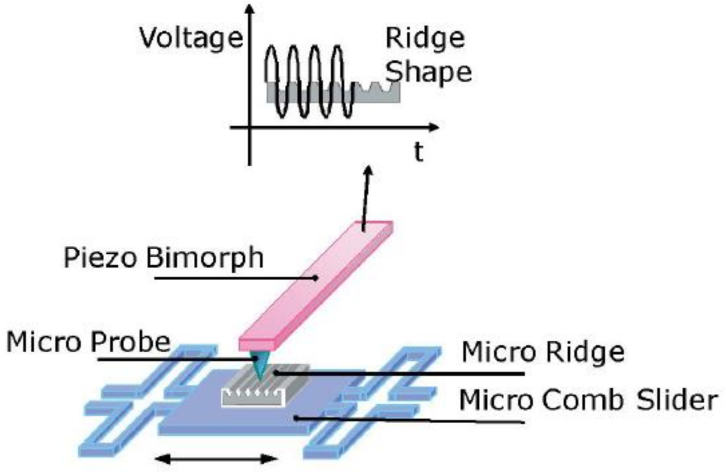

D.G. Lee et al. IEEE porc. (2007)

Impact electrostatic MEMS generator

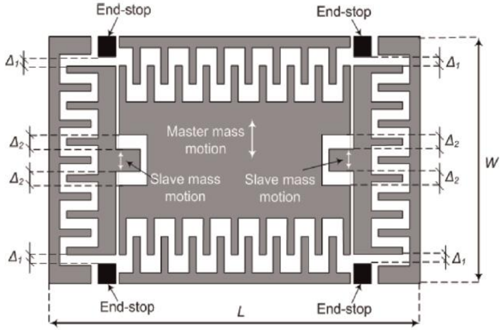

Le, C. P., Halvorsen (2012). *Journal of Intelligent Material Systems and Structures*

Beyond linear harvesting systems

Nonlinear systems

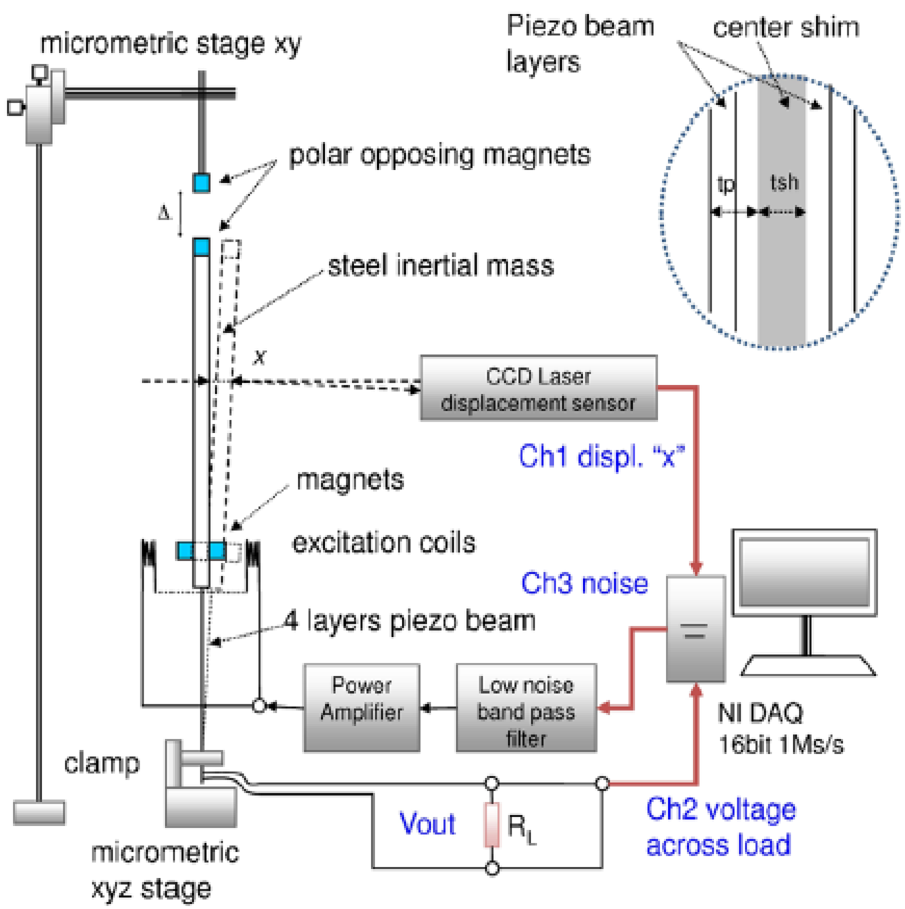

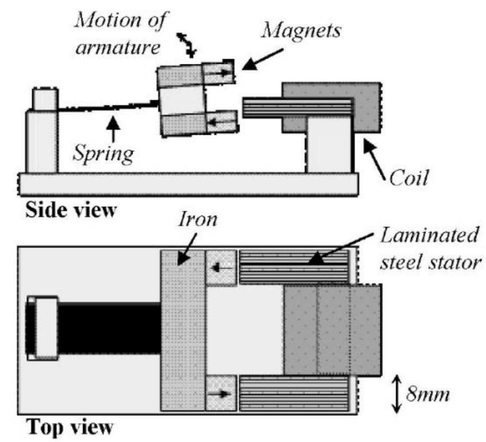

Burrow, S.G and Clare, L.R. IEEE porc. (2007)

Cottone, F., H. Vocca & L. Gammaitoni, Nonlinear Energy Harvesting. *PRL,* 102 (2009).

Beyond linear harvesting systems

Nonlinear systems for vibration energy harvesting

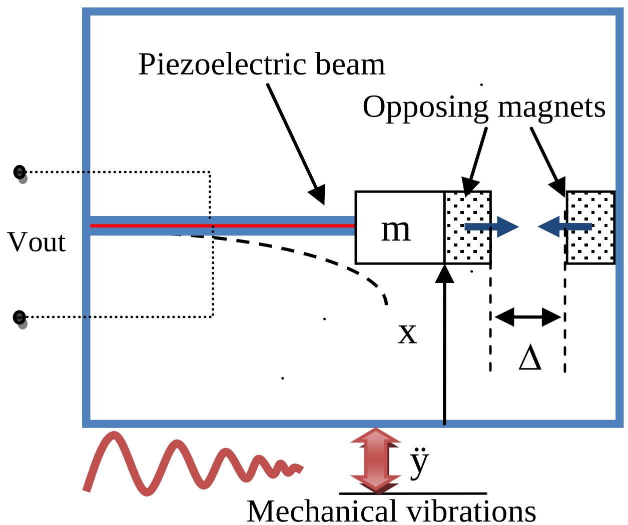

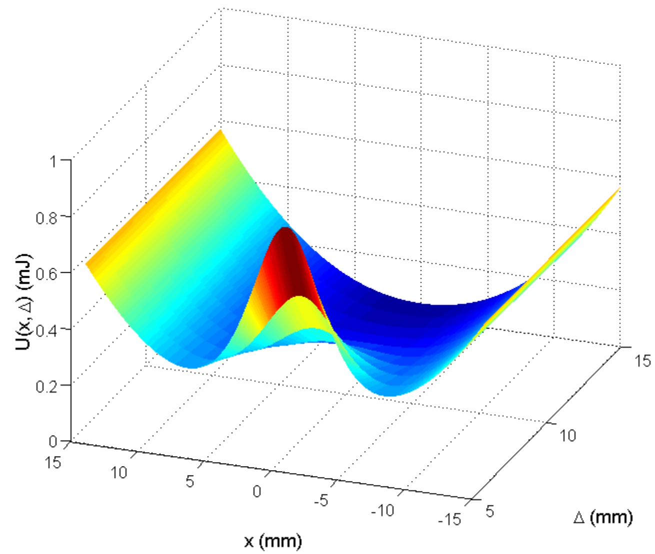

Magneto-elastic potential

$$U(x,\Delta) = \frac{1}{2} K_{eff} x^2 + \frac{\mu_0}{2\pi} \frac{M_1 M_2}{(x^2+\Delta^2)^{3/2}}$$

Governing equations of a single-DOF piezo-magnetoelastic model

$$\begin{cases} m\ddot{x}(t) + \delta \dot{x}(t) + K_{eff} x(t) + \dfrac{\partial U(x,\Delta)}{\partial x} + K_v V(t) = -m\ddot{y}(t) \\ \dot{V}(t) + \dfrac{1}{\tau} V(t) = K_c \dot{x}(t); \qquad \tau = R_L C_p \end{cases}$$

Cottone, F., H. Vocca & L. Gammaitoni. *PRL,* 102 (2009).

Bistable oscillators for vibration energy harvesting

Bistable: inter-well and intra-well oscillations

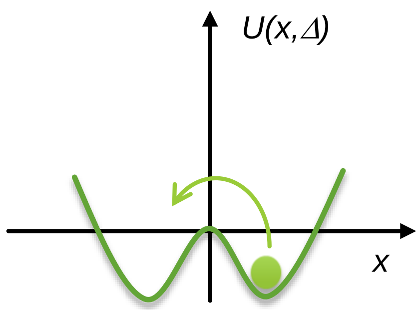

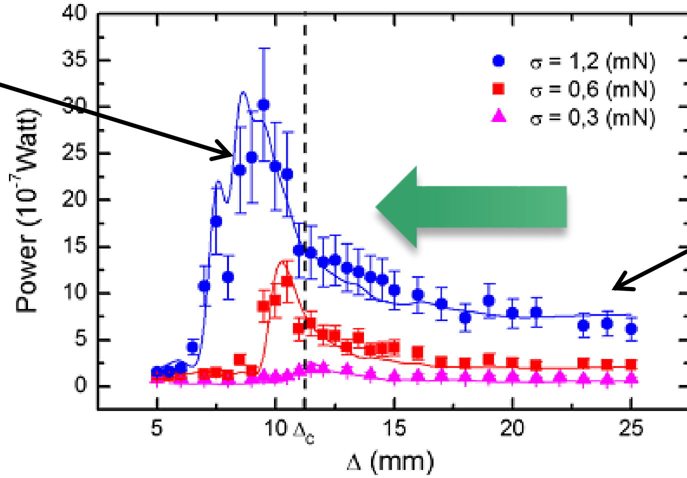

Resonant monostable

Δ=25mm

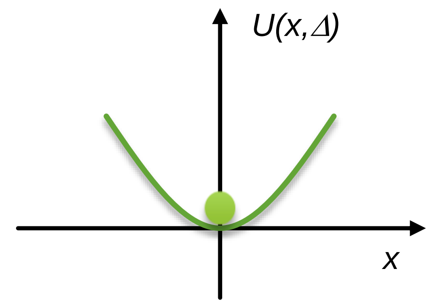

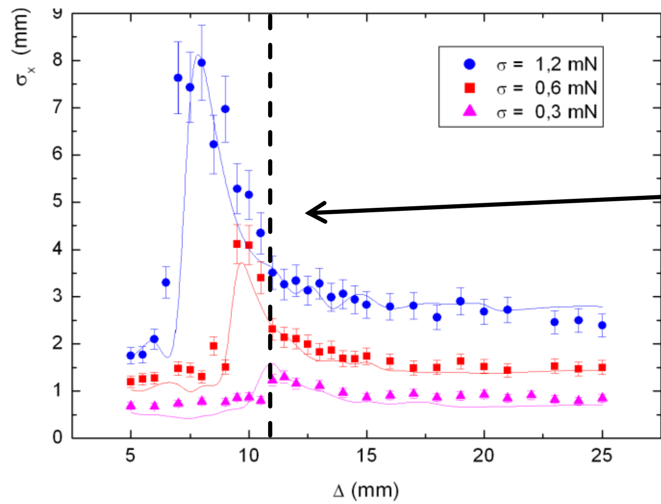

Bifurcation point

Cottone, F., H. Vocca & L. Gammaitoni, Nonlinear Energy Harvesting. *PRL,* 102 (2009).

Bistable oscillators for vibration energy harvesting

Bistable: inter-well and intra-well oscillations

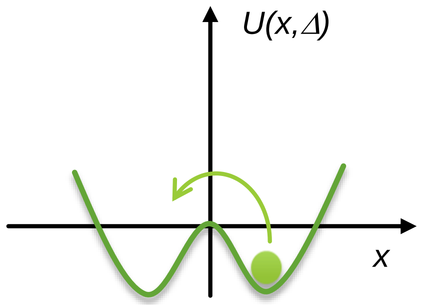

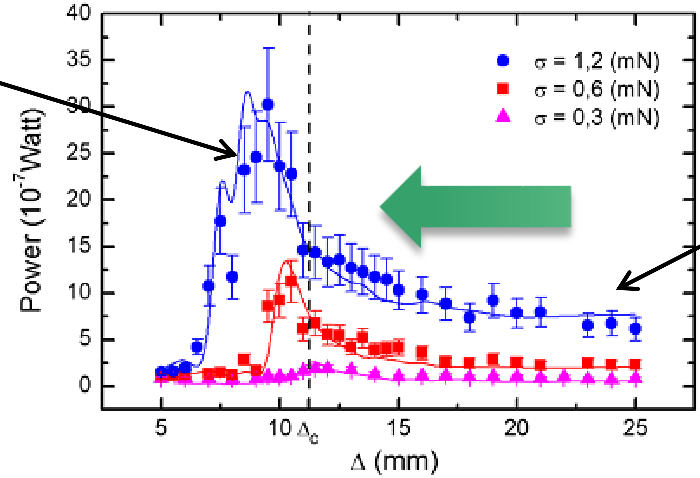

Resonant monostable

Δ=25mm

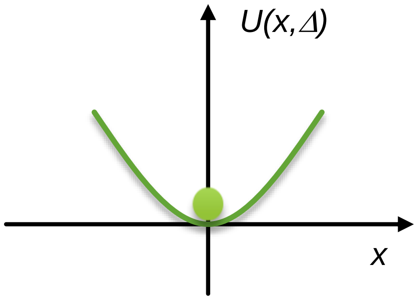

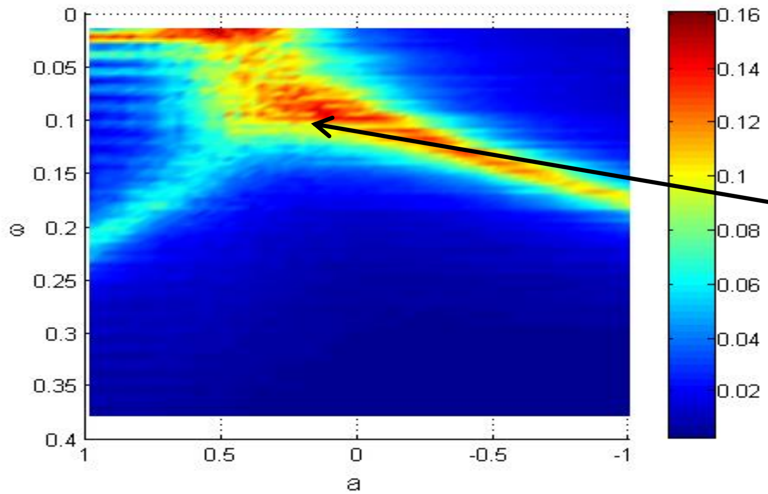

Bandwith enhancement when interwell jumps occur

Bistable oscillators for vibration energy harvesting

Buckled beam piezoelectric harvesters

Cottone, F., Gammaitoni, L., Vocca, H., Ferrari, M., & Ferrari, V. (2012). *Smart materials and structures, 21*(3), 035021

Snapping between buckled states

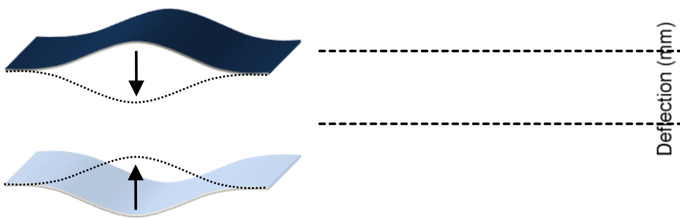

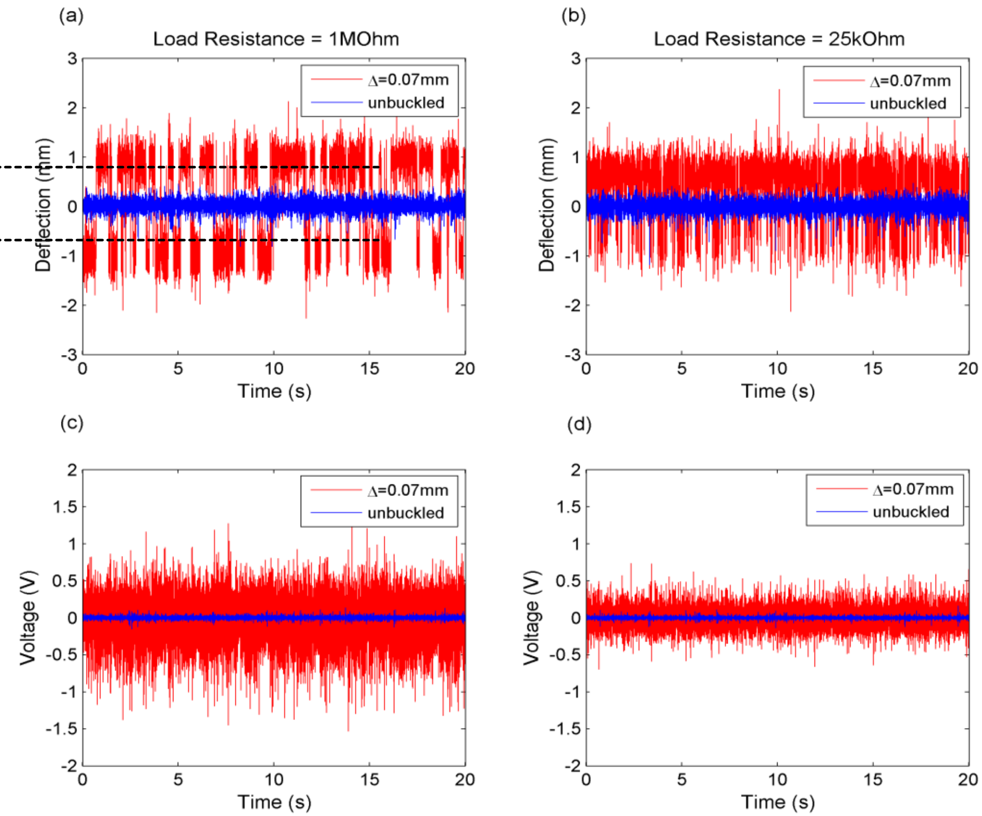

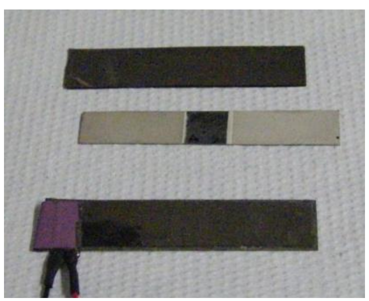

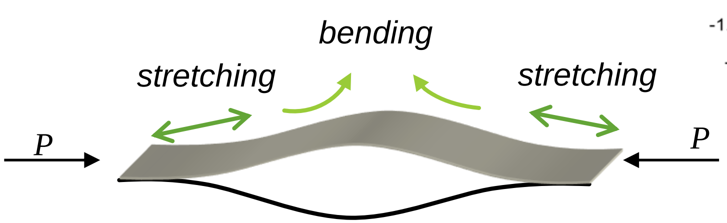

Bistable oscillators for vibration energy harvesting

Buckled piezoelectric beams

$$w(x,t) = w_1(x) + v(x,t)$$

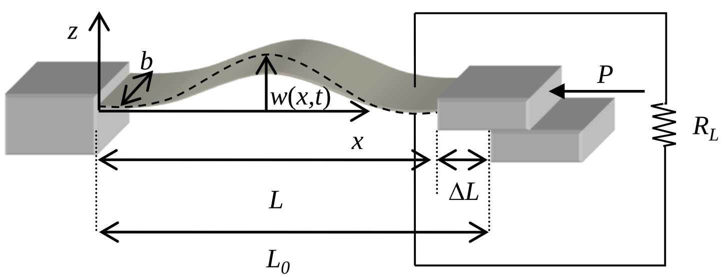

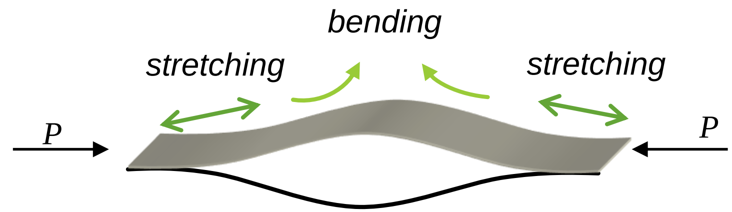

the initial buckling shape function is

$$\psi(x) = h_0(1-\cos(2\pi x / L)) / 2$$

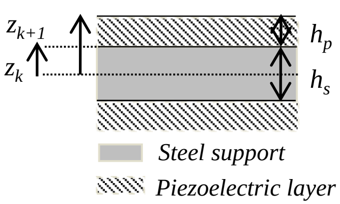

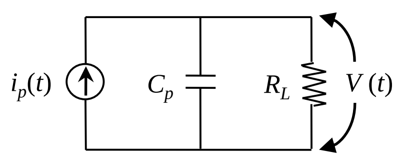

by applying Euler-Lagrange equations

$$\frac{d}{dt}\left(\frac{\partial \mathfrak{L}}{\partial \dot{q}}\right) - \frac{\partial \mathfrak{L}}{\partial q} = F(t), \qquad \frac{d}{dt}\left(\frac{\partial \mathfrak{L}}{\partial \dot{\lambda}}\right) - \frac{\partial \mathfrak{L}}{\partial \lambda} = I(t)$$

gives two coupled second order nonlinear differential equations governing the motion of the piezoelectric buckled beam

$$\begin{cases} m\ddot{q} + c\dot{q} + k_3 q^3 + (k_2 - k_1 V)q + k_0 V = -\eta \ddot{z}, \\ \dot{V} + \dfrac{2}{R_L C_p} V = 2\dfrac{k_0}{C_P}\dot{q} - 2\dfrac{k_1}{C_P} q\dot{q}. \end{cases}$$

Where the output voltage is related to the flux linkage $V = -\dot{\lambda}$

Bistable oscillators for vibration energy harvesting

Experimental and numerical results

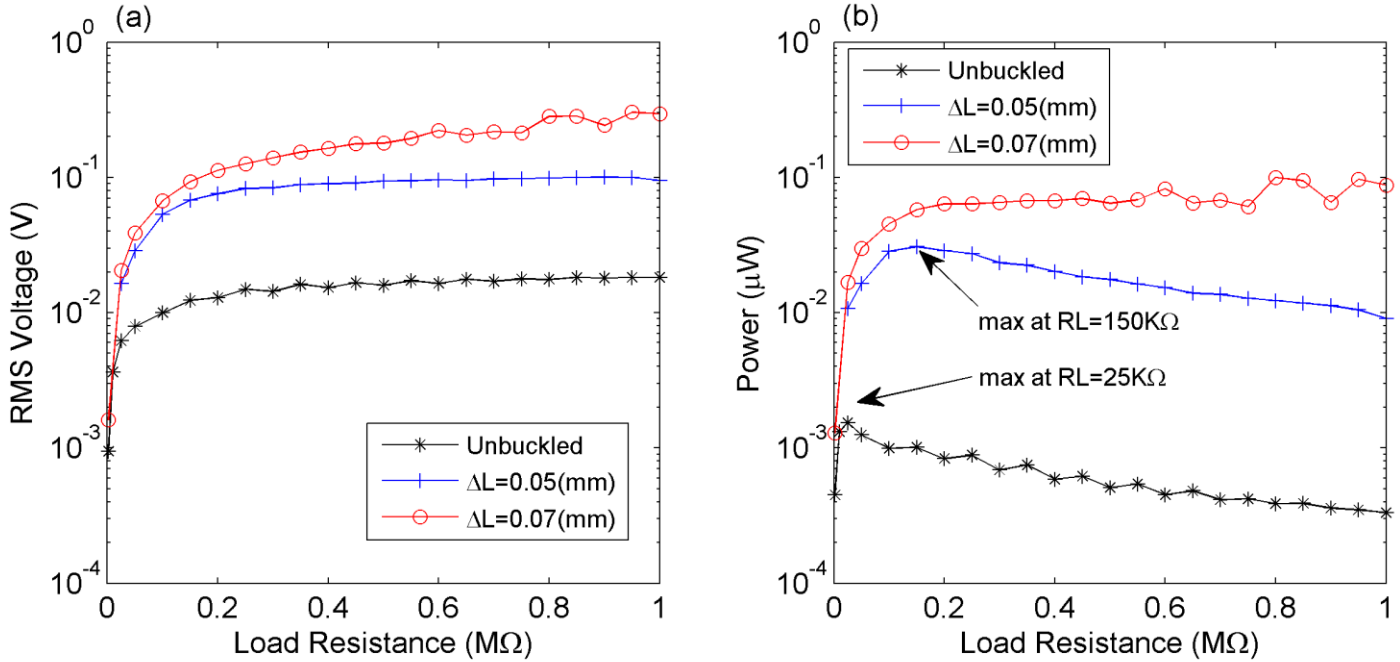

Cottone, F., L. Gammaitoni, H. Vocca, M. Ferrari & V. Ferrari (2012) Smart materials and structures, 21, 2012.

Nonlinear electromagnetic generators for wide band vibrational energy harvesting

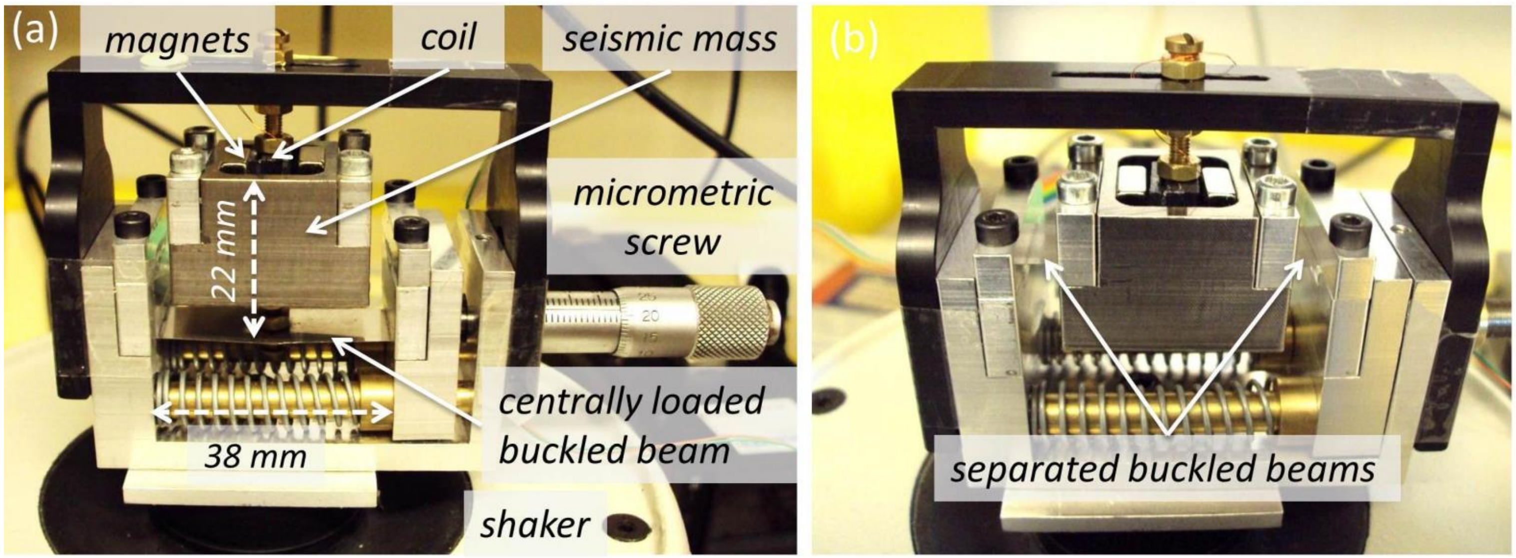

Figure 2. Photographs of the BEMG prototype for the (a) single centrally loaded-beam clamping configuration, (b) double-beam clamping configuration, and (c) scheme of the testing equipment.
BEMG: beam electromagnetic generator; PC: personal computer; DAQ: data acquisition.

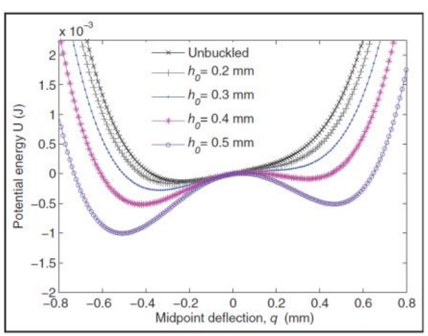

Figure 3. Potential energy of the system for increasing values of buckling height h_0.

$$\frac{d^2\tilde{q}(\tau)}{d\tau^2}+\frac{1}{Q}\frac{d\tilde{q}(\tau)}{d\tau}+\tilde{q}(\tau)+\tilde{q}^3(\tau)+\tilde{V}(\tau)=-\frac{d^2\tilde{y}(\tau)}{d\tau^2},$$

$$\frac{d\tilde{V}(\tau)}{d\tau}+\frac{1}{\gamma}\tilde{V}(\tau)=k_{em}^2\frac{d\tilde{q}}{d\tau},$$

$$\gamma=\omega_0/(\omega_R+\omega_L) \qquad k_{em}^2=\frac{\lambda^2}{k_1L_c}=\frac{(Bl)^2}{k_1L_c}. \qquad k_{pz}^2=\frac{\alpha^2}{k_1C_0}$$

Nonlinear electromagnetic generators for wide band vibrational energy harvesting

Bandwidth enhancement of 2.5x with bistability at 0,2 grms

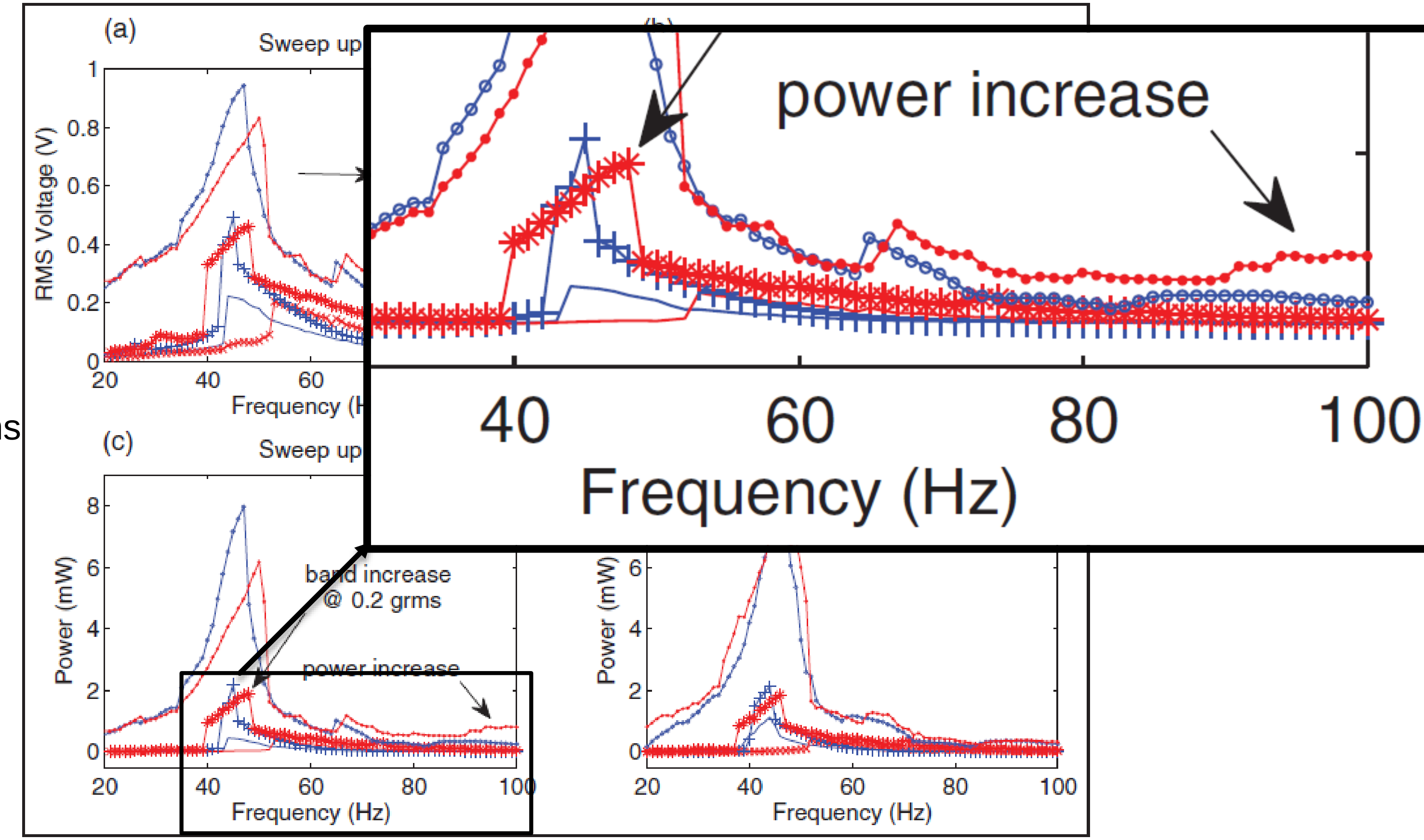

Figure 6. Experimental comparison of unbuckled- and buckled-beam (h_0 = 0.3 mm) generators for up (left column) and down (right column) frequency sweeps with acceleration amplitudes of 0.1, 0.2, and 0.5 g_{rms}. (a and b) *rms* voltage and (c and d) the corresponding power dissipated across the optimal load resistance R_L = 112 Ω.

rms: root mean square.

MEMS electrostatic kinetic energy harvester

Université Paris-Est, ESIEE Paris,
Silicon MEMS electrostatic harvesters.

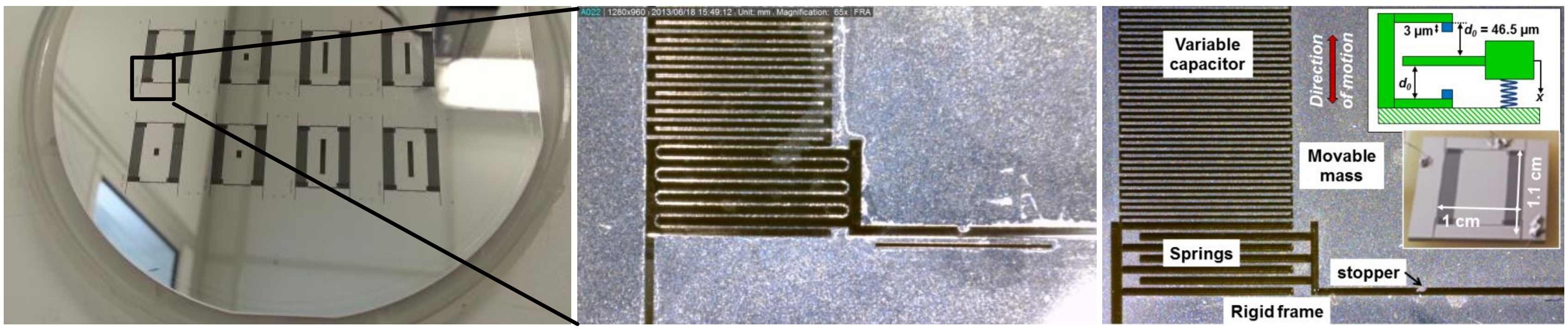

- **Cottone, F.,** Basset, P., Guillemet, R., Galayko, D., Marty, F. and T. Bourouina. IEEE TRANSDUCERS 2013.
- R., Guillemet, Basset., P, Galayko, D., **Cottone, F**., Marty, F. and T. Bourouina. Conf. Proceeding IEEE MEMS 2013.

MEMS electrostatic kinetic energy harvester

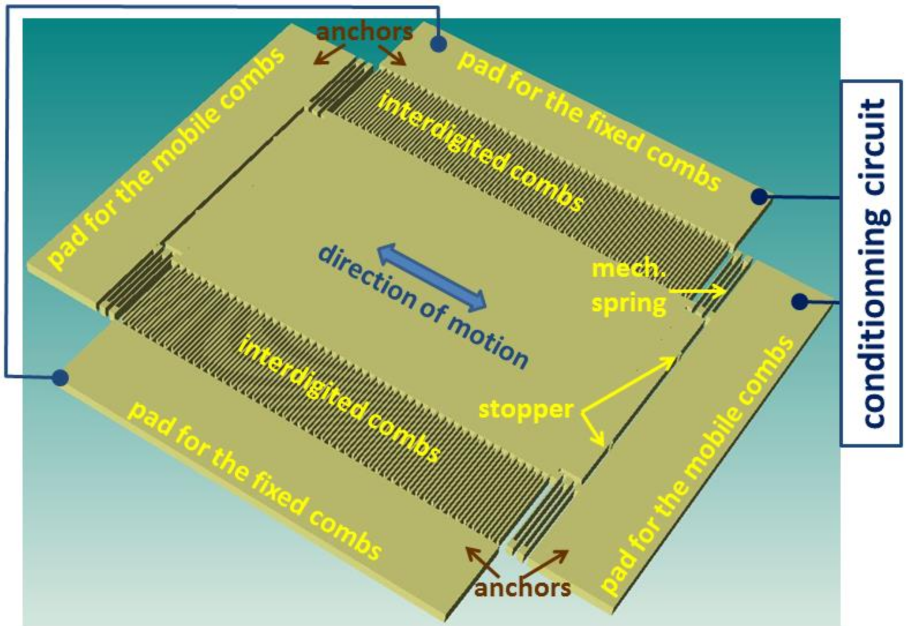

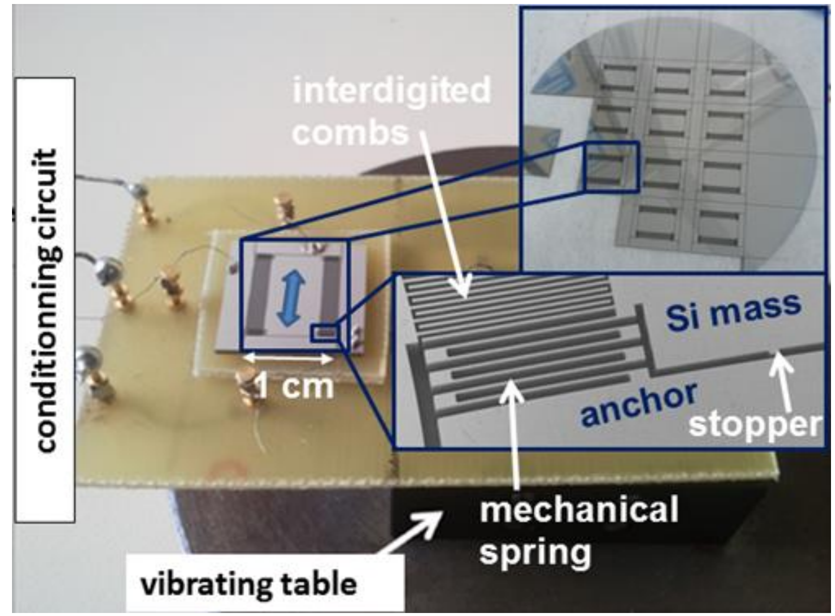

Guilllemet, R., Basset, P., Galayko, D., Cottone, F., Marty, F., & Bourouina, T. (2013). *Micro Electro Mechanical Systems (MEMS), 2013 IEEE 26th International Conference on* (pp. 817-820): IEEE.

Cottone, F., Basset, P., Guillemet, R., Galayko, D., Marty, F., & Bourouina, T. (2013). *2013 Transducers & Eurosensors.*

Basset, P., Galayko, D., Cottone, F., Guillemet, R., Blokhina, E., Marty, F., & Bourouina, T. (2014). *Journal of Micromechanics and Microengineering 24(3), 035001*

MEMS electrostatic kinetic energy harvester

F. Cottone, P. Basset Université Paris-Est, ESIEE Paris,
Silicon MEMS-based electrostatic harvesters.

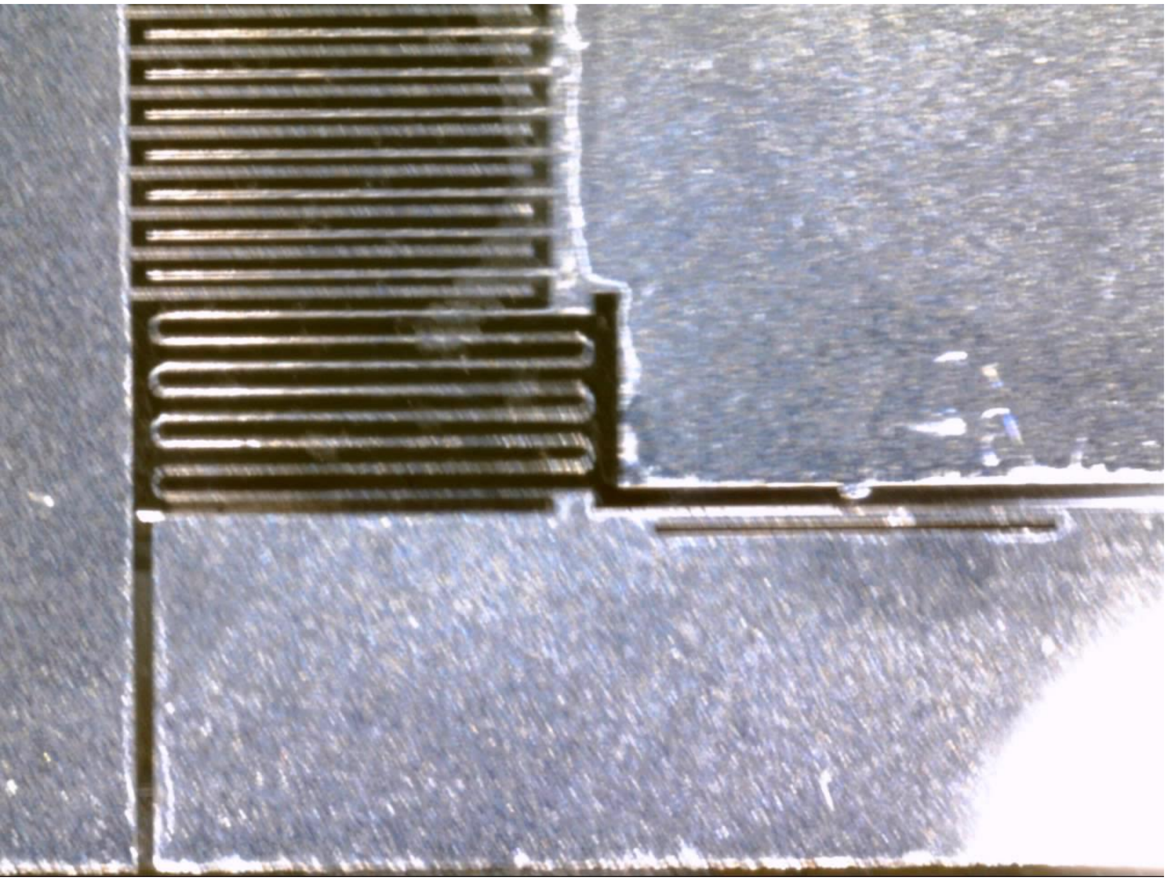

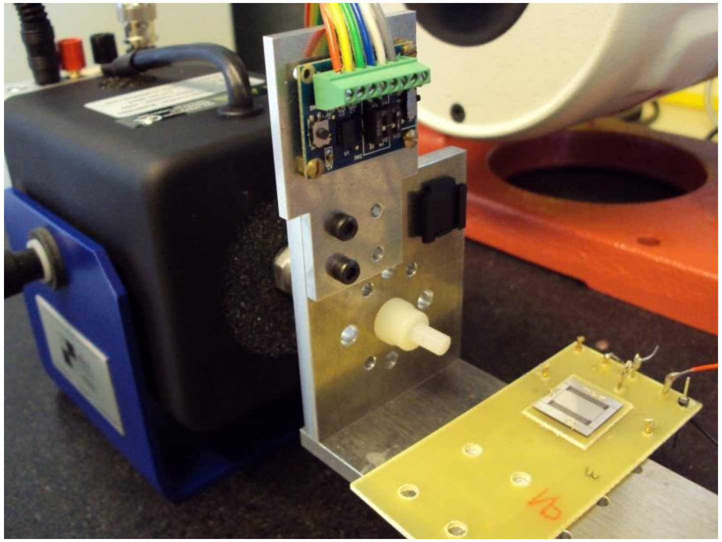

MEMS electrostatic kinetic energy harvester

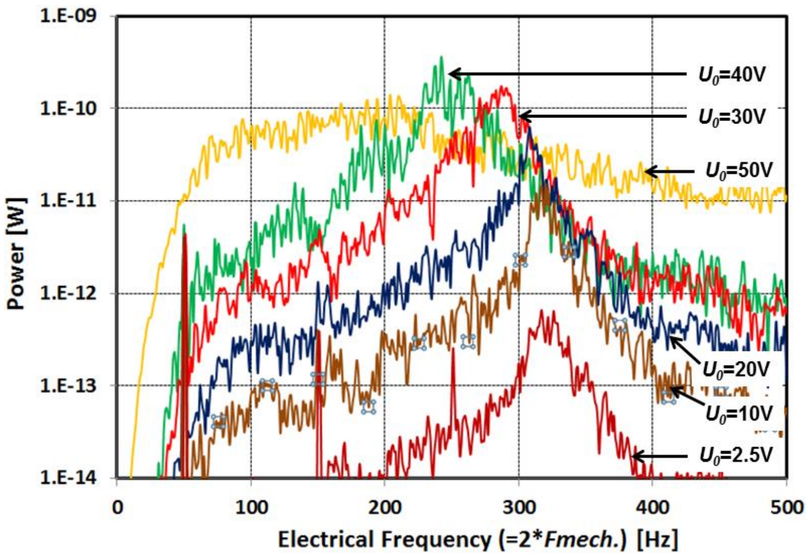

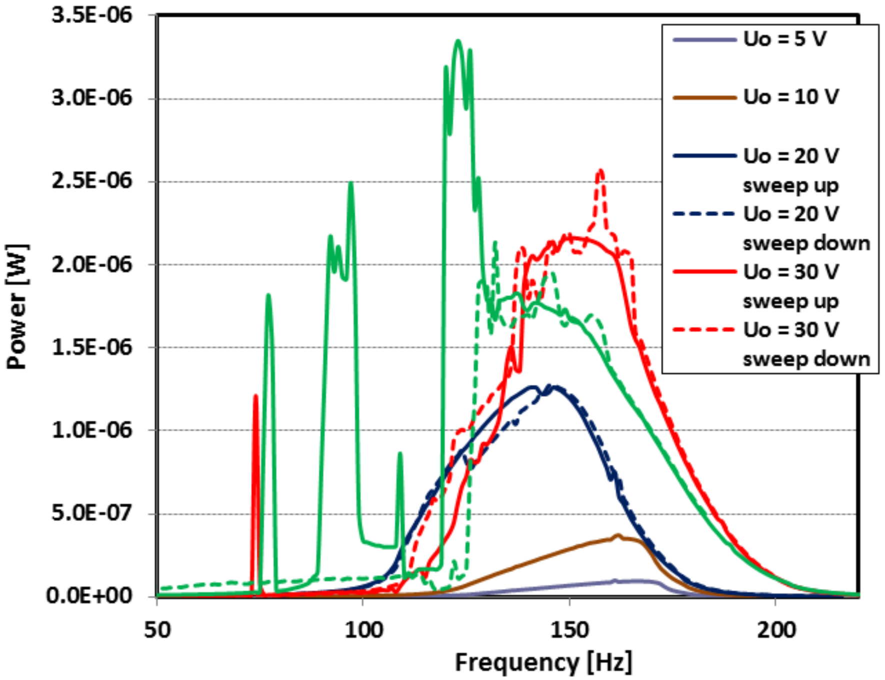

Cottone, F., Basset, P., Guillemet, R., Galayko, D., Marty, F., & Bourouina, T. (2013). *Transducers & Eurosensors.*

Basset, P., Galayko, D., Cottone, F., Guillemet, R., Blokhina, E., Marty, F., & Bourouina, T. (2014). JMM *24*(3), 035001.

Electromagnetic generators

Velocity-amplified mulitple-mass EM VEH

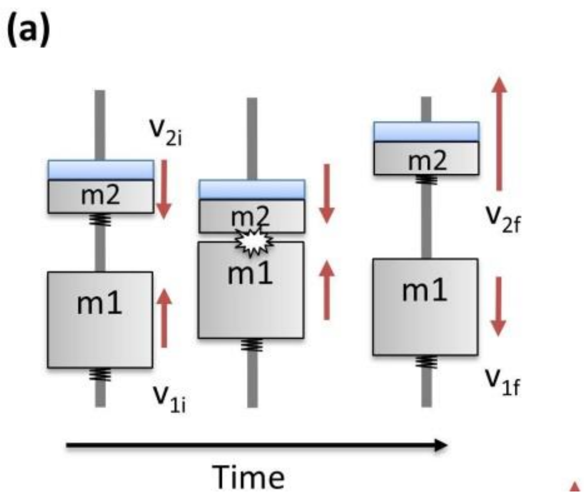

$$v_{2f} = \frac{(e+1)m_1 v_{1i} + (m_2 - em_1)v_{2i}}{m_1 + m_2}$$

if e = 1 and in the limit of $m_1 / m_2 \rightarrow \infty$,

the final velocity of the smaller mass is

$$v_{2f} = 2v_{1f} - v_{2i}.$$

In the case of equal but opposite initial velocities

$$v_{2f} = -3v_{2i},$$

which represents a gain **factor of 3x** in velocity.

Electromagnetic generators

Velocity-amplified mulitple-mass EM VEH

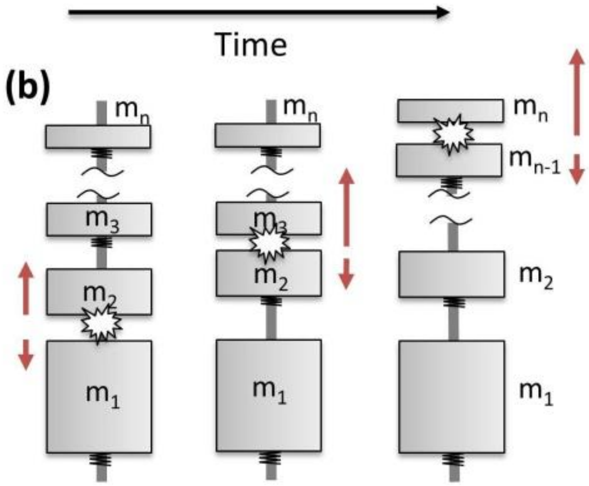

For a series of n−bodies of progressively smaller mass that impact sequentially, the velocity gain is proportional to n.
(Rodgers et al., 2008)

$$G_n = (1 + e_{1,0}) \prod_{k=2}^{n} \left(\frac{1 + e_{k,k-1}}{1 + r_{k,k-1}} \right) - 1$$

Electromagnetic generators

Velocity-amplified mulitple-mass EM VEH

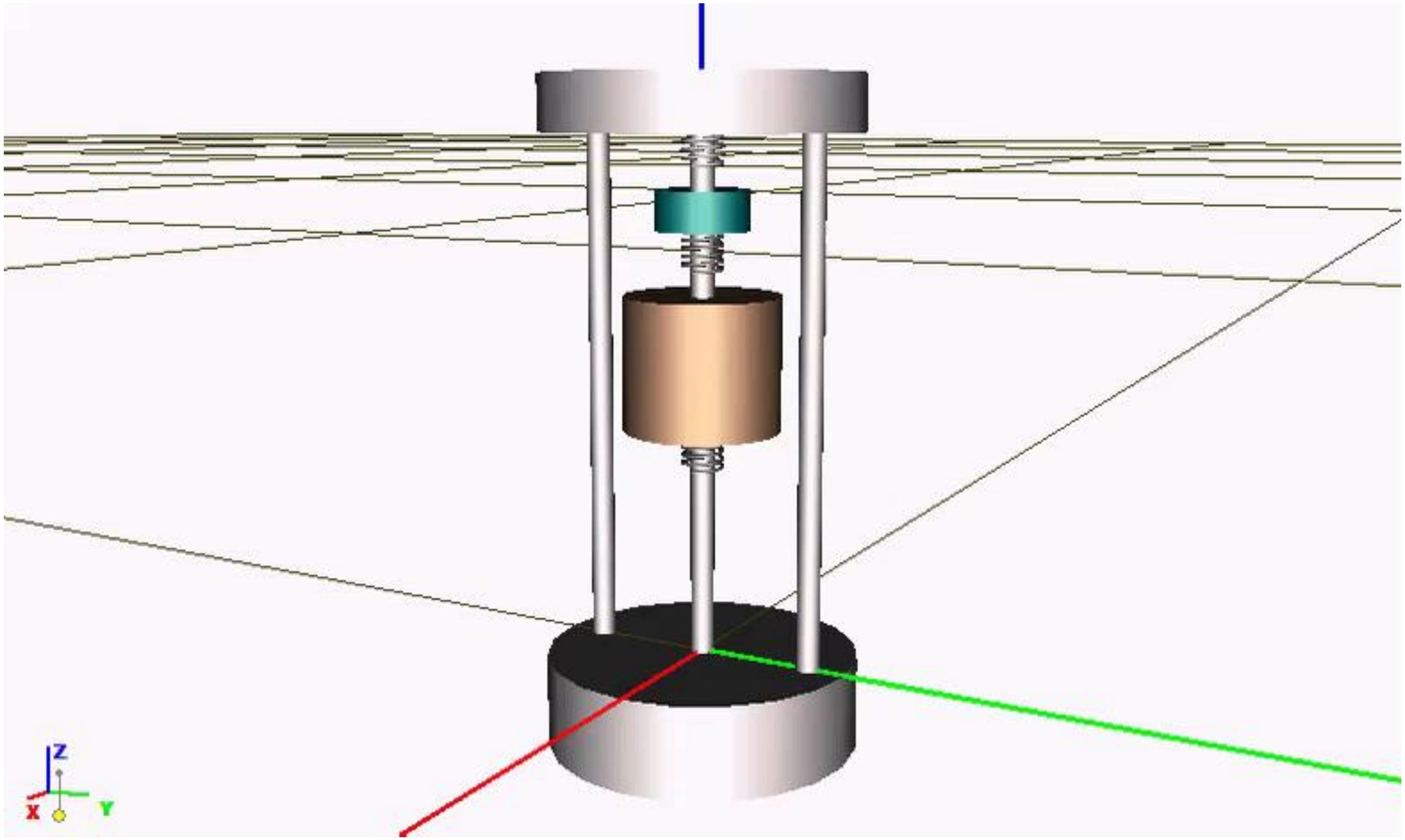

Electromagnetic generators

Velocity-amplified mulitple-mass EM VEH

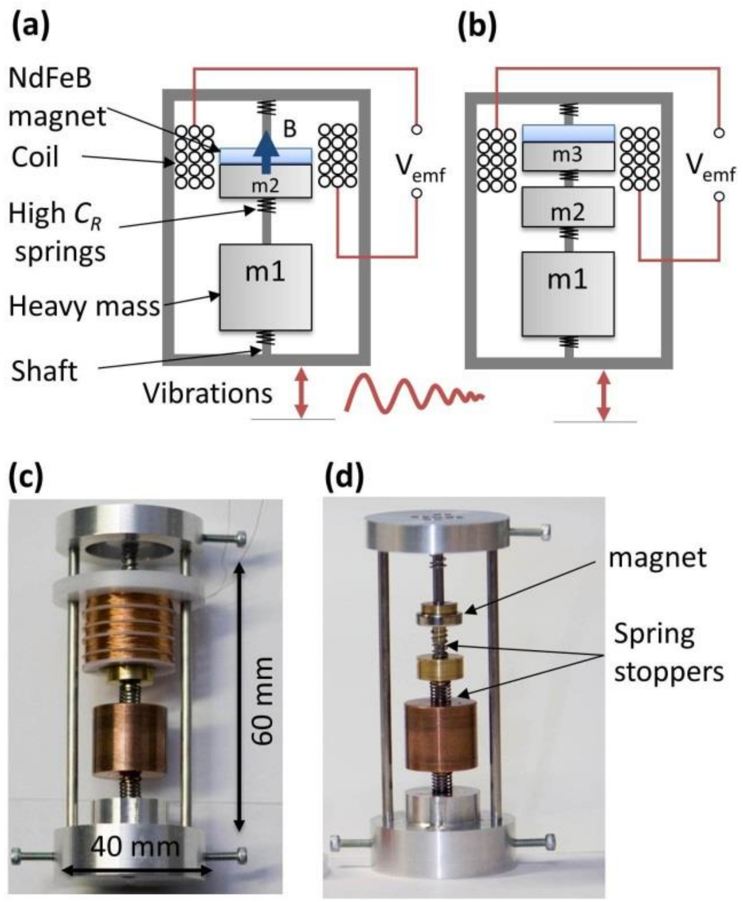

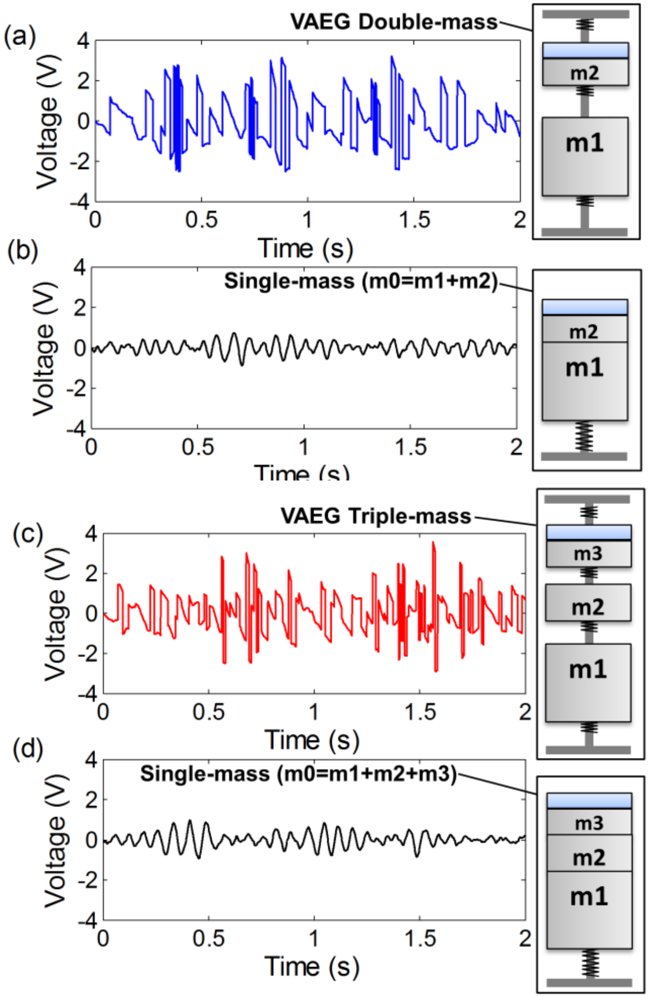

Electromagnetic generators

Velocity-amplified mulitple-mass EM VEH

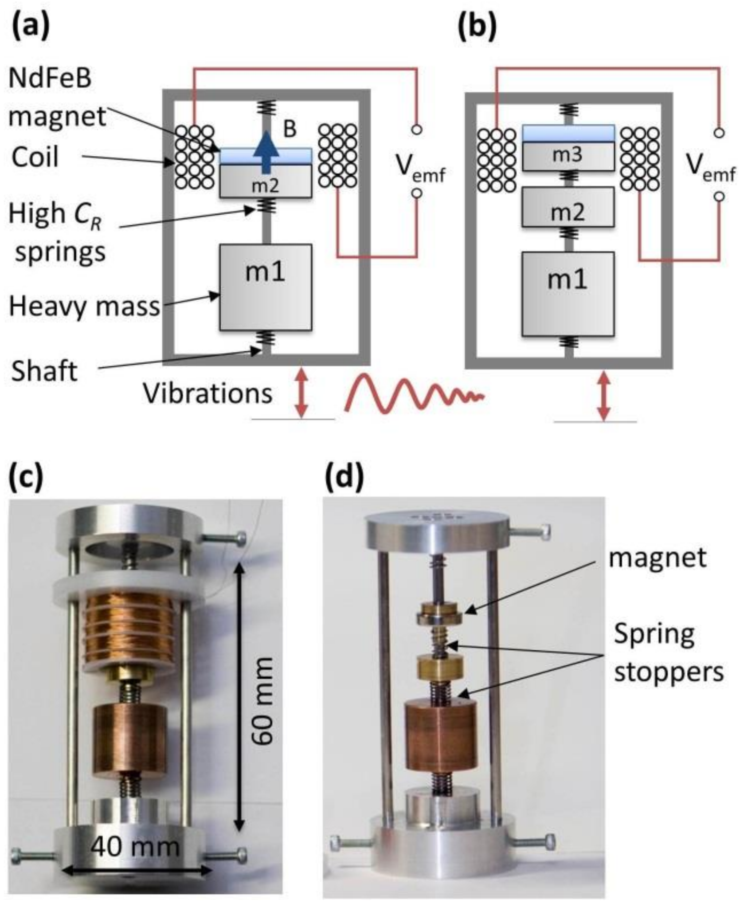

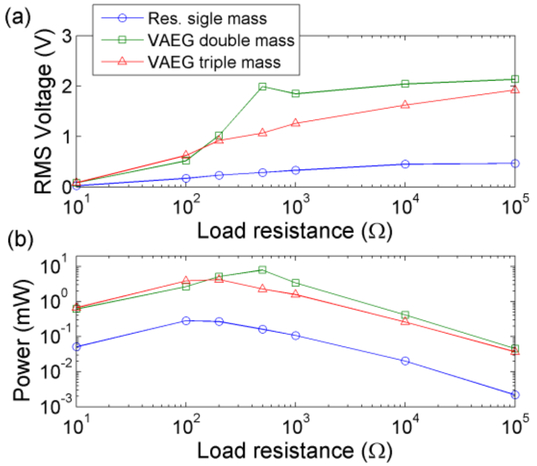

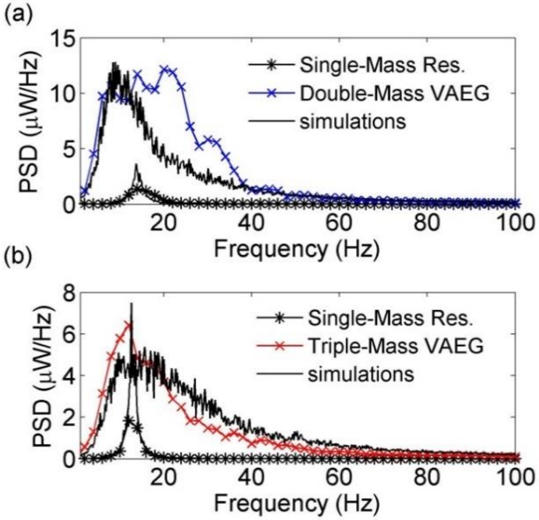

Electromagnetic generators

Velocity-amplified mulitple-mass EM VEH

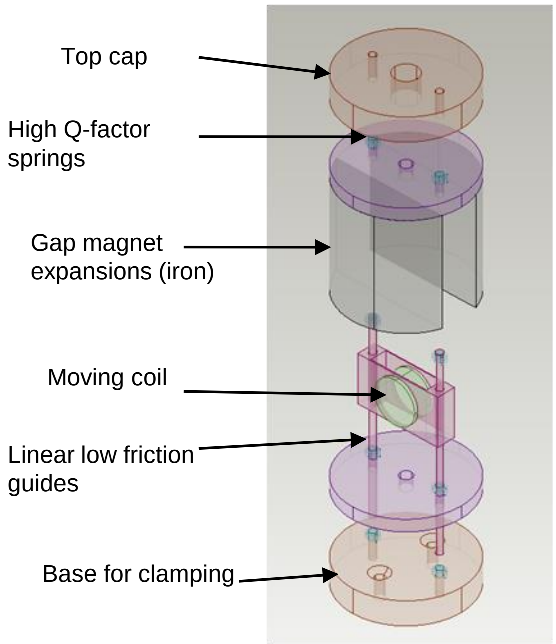

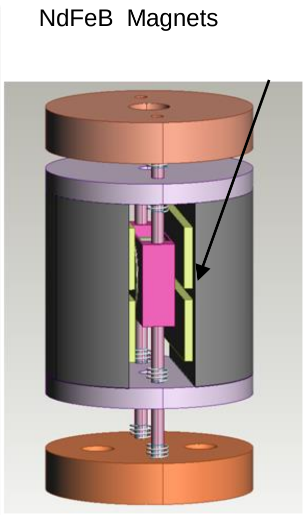

Prototype 2 with transversal magnetic flux

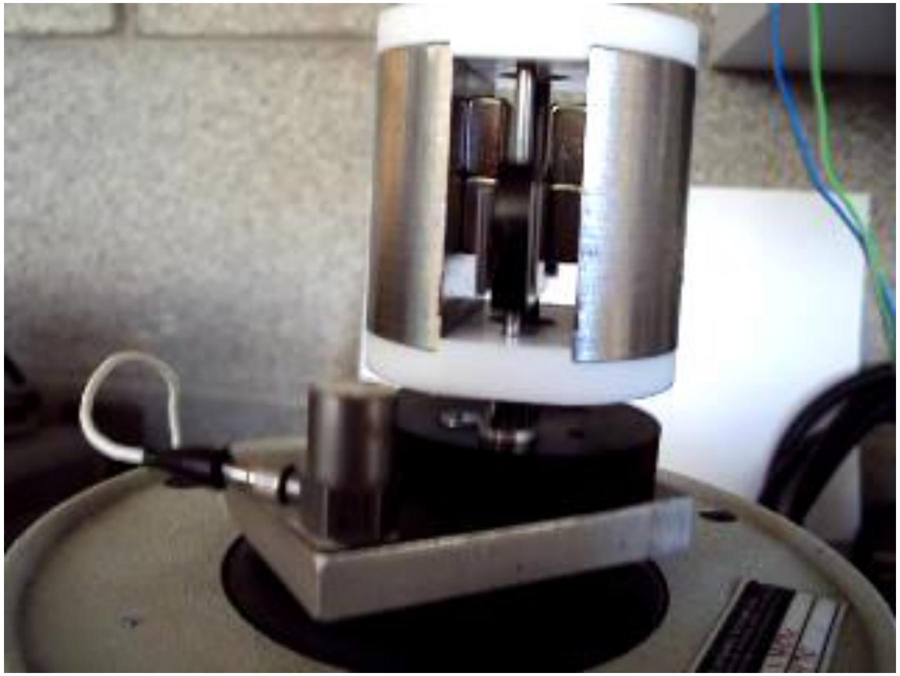

University of Limerick (Ireland) and Bell-Labs Alcatel (USA).

F. Cottone, G. Suresh, J. Punch - "*Energy Harvesting Apparatus Having Improved Efficiency*". US Patent n. 8350394B2

Electromagnetic generators

Velocity-amplified mulitple-mass EM VEH

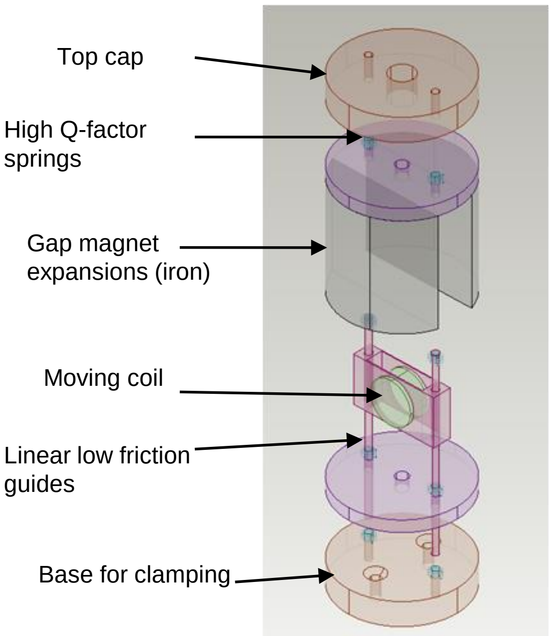

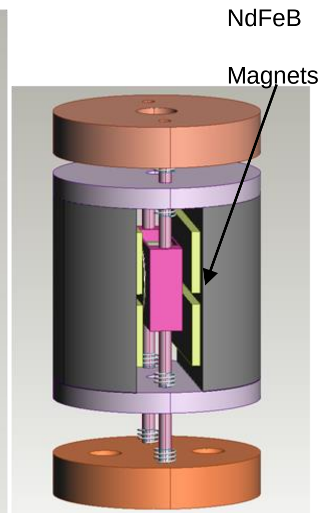

Prototype 2 with transversal flux linkage

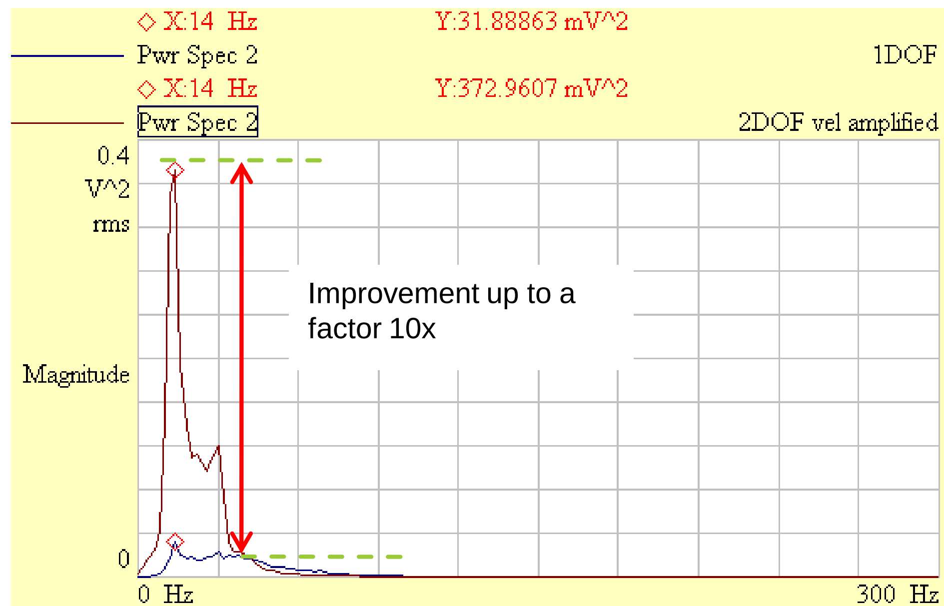

University of Limerick (Ireland) and Bell-Labs Alcatel (USA).

F. Cottone, G. Suresh, J. Punch - "*Energy Harvesting Apparatus Having Improved Efficiency*". US Patent n. 8350394B2

Comparison of various approaches

Strategies	Advantages	Disadvantages
Mechanical tuning	• High efficiency	• Extra system and energy are required • Responds to only one frequency at a time • Slow response to a change in a vibration frequency
• Change dimension	• Does not affect damping	• Difficult to implement • Not suitable for tuning *in situ*[a]
• Change centre of gravity	• Does not affect damping	• Not suitable for tuning *in situ*
• Change spring stiffness continuously	• Suitable for *in situ* tuning	• Consumes energy when generators work at resonance
• Apply axial load (change spring stiffness intermittently)	• Easy to implement • Suitable for *in situ* tuning • No energy is required when generators work at resonance • Damping is not affected when the tensile load is applied	• Increased damping when the compressive load is applied
Electrical tuning	• Easy to implement • No energy is required when generators work at resonance • Suitable for *in situ* tuning	• Low tuning efficiency
Widen bandwidth	• No tuning mechanism required • Respond to different frequencies at the same time • Immediate response to a change in vibration frequency	• Complexity in design
• Generator array	• Damping is not affected	• Complexity in design • Low volume efficiency
• Use mechanical stopper	• Easy to implement	• Fatigue problem • Decrease in the maximum output power
• Coupled oscillators	• Easy to implement	• Decrease in the maximum output power
• Nonlinear generators	• Better performance at excitation frequencies higher than resonant frequency	• Complexity in design • Hysteresis
• Bi-stable structure	• Better performance at excitation frequencies much lower than resonant frequency	• Complexity in design

[a] Tuning while the generator is mounted on the vibration source and working.

Zhu, D., Tudor, M. J., & Beeby, S. P. (2010).

Performance metrics

$$\mathrm{FoM_V} = \frac{\text{Useful Power Output}}{\frac{1}{16} Y_0 \rho_{Au} Vol^{\frac{4}{3}} \omega^3}$$

Bandwidth figure of merit

$$\mathrm{FoM_{BW}} = \mathrm{FoM_V} \times \frac{\delta\omega_{1\ \mathrm{dB}}}{\omega}$$

Frequency range within which the output power is less than 1 dB below its maximum value

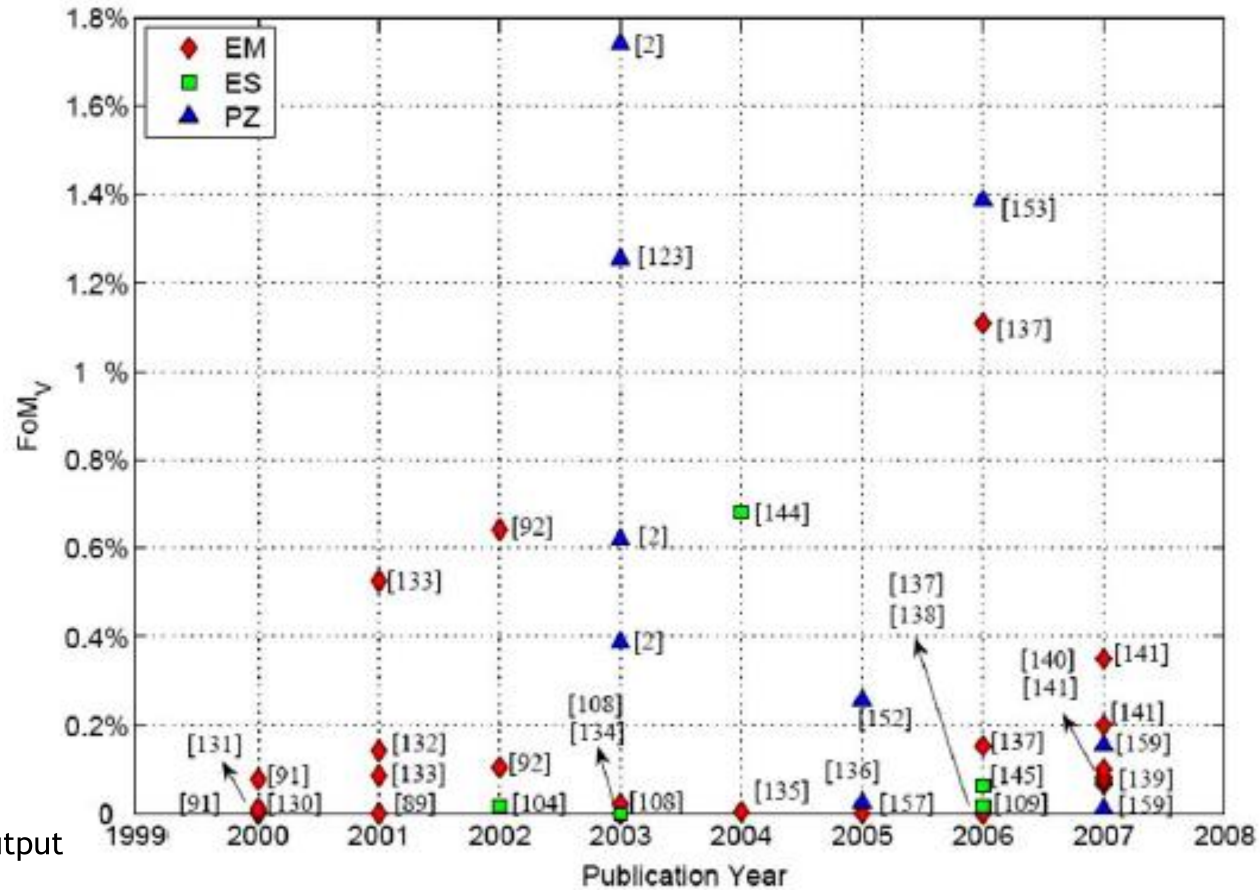

Mitcheson, P. D., E. M. Yeatman, et al. (2008). Proceedings of the IEEE **96**(9): 1457-1486.

Conclusions

- Marriage between Energy harvesting systems and Zero-power Technology will enable autonomous WSN applications

- Energy harvesting systems can be improved by:
  - Nonlinear dynamic: Bistable systems, freqeuncy-up converters, impacting masses, electrostatic softening
  - Innovative electro-active materials (electrets, lead-free piezo)
  - Miniaturization

- Zero-Power Technology has plenty of room for improvement at level of
  - Low-consumption components,
  - Efficient conditioning.

Current technical challenges

- **Miniaturization issues**
  - Improvements of piezoelectric-material properties
  - Improving capacitive design
  - Increasing magnetic filed in micro magnets
  - Research on electrets materials

- **Efficient conditioning electronics**
  - Efficient Integrated design
  - Power-aware operation of the powered device

- **Target applications**
  - Tailoring the WSN technology to specific applications

Acknowledgments

Thank you

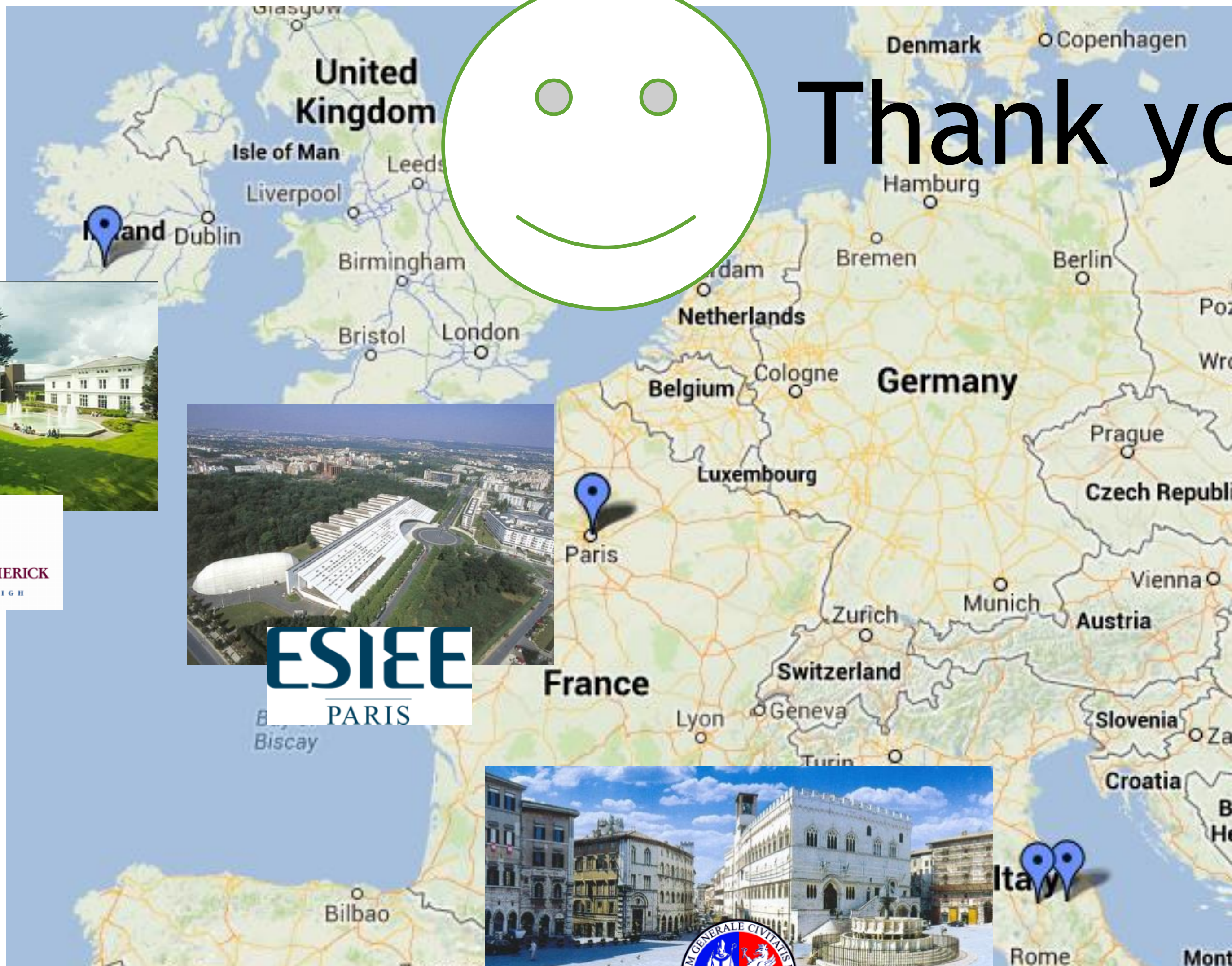

UNIVERSITY of LIMERICK
OLLSCOIL LUIMNIGH

ESIEE
PARIS